The Star Formation Newsletter

A community newsletter on Star and Planet Formation research

No. 367 — 31 July 2023
Editor: João Alves
www.starformation.news

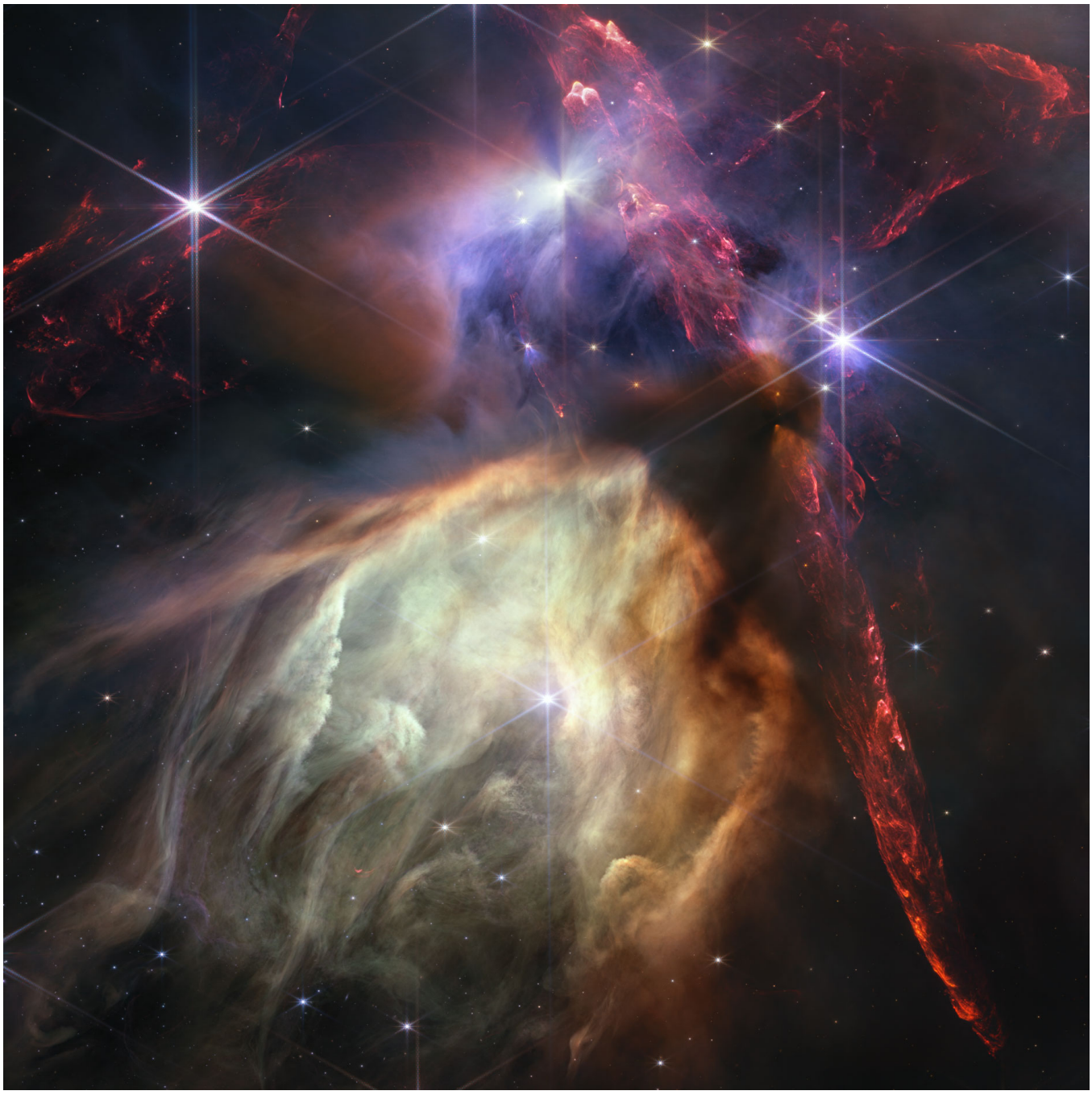

Links to sections

Cover image caption

Nebula around Oph S1 star, the closest and youngest early B-star (B3) as observed by JWST. The lighter-coloured gas nebula surrounding S1 consists of polycyclic aromatic hydrocarbons and has a diameter of about 0.1 pc. The nebula is located towards the northern region of dense cloud L1688, in Ophiuchus, at a distance of about 145 pc. In the top half of the image, (at least) two HH-object systems shoot out from young stars, and several disk shadows can be seen.

Credits: NASA, ESA, CSA, STScI, K. Pontoppidan (STScI), A. Pagan (STScI)

Note from the Editor

The Star Formation Newsletter is now on the web at **www.starformation.news**. This PDF file contains the monthly Abstracts and links to the different Newsletter sections. Red text in this PDF is a url link. Submitting an abstract to the SFN is as simple as entering the arXiv ID (e.g., 2006.10139) in a web form on the SFN web site. **Do not remove the LaTeX formatting when submitting to the arXiv**. If you do, your abstract will not look great either at the arXiv or the SFN.

Abstracts

1. ## Coagulation-Fragmentation Equilibrium for Charged Dust: Abundance of Submicron Grains Increases Dramatically in Protoplanetary Disks

Vitaly Akimkin, Alexei V. Ivlev, Paola Caselli, Munan Gong, Kedron Silsbee ★ Dust coagulation in protoplanetary disks is not straightforward and is subject to several slow-down mechanisms, such as bouncing, fragmentation and radial drift to the star. Furthermore, dust grains in UV-shielded disk regions are negatively charged due to collisions with the surrounding electrons and ions, which leads to their electrostatic repulsion. For typical disk conditions, the relative velocities between micron-size grains are small and their collisions are strongly affected by the repulsion. On the other hand, collisions between pebble-size grains can be too energetic, leading to grain fragmentation. The aim of the present paper is to study a combined effect of the electrostatic and fragmentation barriers on dust evolution. We numerically solve the Smoluchowski coagulation-fragmentation equation for grains whose charging occurs under conditions typical for the inner disk regions, where thermal ionization operates. We find that dust fragmentation efficiently resupplies the population of small grains under the electrostatic barrier. As a result, the equilibrium abundance of sub-micron grains is enhanced by several orders of magnitude compared to the case of neutral dust. For some conditions with fragmentation velocities ~ 1 m s^{-1}, macroscopic grains are completely destroyed.

2. ## The distribution of accretion rates as a diagnostic of protoplanetary disc evolution

R. Alexander, G. Rosotti, P. J. Armitage, G. J. Herczeg, C. F. Manara, B. Tabone ★ We show that the distribution of observed accretion rates is a powerful diagnostic of protoplanetary disc physics. Accretion due to turbulent ("viscous") transport of angular momentum results in a fundamentally different distribution of accretion rates than accretion driven by magnetised disc winds. We find that a homogeneous sample of $\gtrsim$300 observed accretion rates would be sufficient to distinguish between these two mechanisms of disc accretion at high confidence, even for pessimistic assumptions. Current samples of T Tauri star accretion rates are not this large, and also suffer from significant inhomogeneity, so both viscous and wind-driven models are broadly consistent with the existing observations. If accretion is viscous, the observed accretion rates require low rates of disc photoevaporation ($\lesssim 10^{-9} M_\odot yr^{-1}$). Uniform, homogeneous surveys of stellar accretion rates can therefore provide a clear answer to the long-standing question of how protoplanetary discs accrete.

3. Milliarcsecond structure and variability of methanol maser emission in three high-mass protostars

A Aberfelds, A Bartkiewicz, M Szymczak, J Šteinbergs, G Surcis, A Kobak, M Durjasz, I Shmeld ★ The variability study of 6.7 GHz methanol masers has become a useful way to improve our understanding of the physical conditions in high-mass star-forming regions. Based on the single-dish monitoring using the Irbene telescopes, we selected three sources with close sky positions. We imaged them using the European Very Long Baseline Interferometer Network and searched available data on VLBI archives to follow detailed changes in their structures and single maser spot variability. All three targets show a few groups of maser cloudlets of a typical size of 3.5 mas and the majority of them show linear or arched structures with velocity gradients of order 0.22 km/s,mas^{-1}. The cloudlets and overall source morphologies are remarkably stable on time scales of 7-15 yr supporting a scenario of variability due to changes in the maser pumping rate.

4. The abundance and excitation of molecular anions in interstellar clouds

M. Agundez, N. Marcelino, B. Tercero, I. Jimenez-Serra, J. Cernicharo ★ We report new observations of molecular anions with the Yebes 40m and IRAM 30m telescopes toward the cold dense clouds TMC-1 CP, Lupus-1A, L1527, L483, L1495B, and L1544. We detected for the first time C3N- and C5N- in Lupus-1A and C4H- and C6H- in L483. In addition, we report new lines of C6H- toward the six targeted sources, of C4H- toward TMC-1 CP, Lupus-1A, and L1527, and of C8H- and C3N- in TMC-1 CP. Excitation calculations indicate that the lines of anions accessible to radiotelescopes run from subthermally excited to thermalized as the size of the anion increases, with the degree of departure from thermalization depending on the H2 volume density and the line frequency. We noticed that the collision rate coefficients available for the radical C6H cannot explain various observational facts, which advises for a revisitation of the collision data for this species. The observations presented here, together with observational data from the literature, are used to model the excitation of interstellar anions and to constrain their abundances. In general, the anion-to-neutral ratios derived here agree within 50% (a factor of two at most) with literature values, when available, except for the C4H-/C4H ratio, which shows higher differences due to a revision of the dipole moment of C4H. From the set of anion-to-neutral abundance ratios derived two conclusions can be drawn. First, the C6H-/C6H ratio shows a tentative trend in which it increases with increasing H2 density, as expected from theoretical grounds. And second, it is incontestable that the higher the molecular size the higher the anion-to-neutral ratio, which supports a formation mechanism based on radiative electron attachment. Nonetheless, calculated rate coefficients for electron attachment to the medium size species C4H and C3N are probably too high and too low, respectively, by more than one order of magnitude.

5. Laboratory modeling of jets from young stars using plasma focus facilities

V. S. Beskin, V. I. Krauz, S. A. Lamzin ★ Jets from young stars are used as an example to review how laboratory modeling enables advancement in understanding the main physical processes responsible for the formation and stability of these amazing objects. The discussion focuses on the options for modeling jet emissions in a laboratory experiment at the PF-3 facility at the National Research Center Kurchatov Institute. Many properties of the flows obtained using this experimental setup are consistent with the main features of jets from young stars.

6. Tentative co-orbital submillimeter emission within the Lagrangian region L5 of the protoplanet PDS 70 b

Olga Balsalobre-Ruza, Itziar de Gregorio-Monsalvo, Jorge Lillo-Box, Nuria Huélamo, Álvaro Ribas, Myriam Benisty, Jaehan Bae, Stefano Facchini, Richard Teague ★ Context: High-spatial resolution Atacama Large Millimeter/submillimeter Array (ALMA) data have revealed a plethora of substructures in protoplanetary disks. Some of those features are thought to trace the formation of embedded planets. One example is the gas and dust that accumulated in the co-orbital Lagrangian regions L_4/L_5, which were tentatively detected in recent years and might be the pristine material for the formation of Trojan bodies. Aims: This work is part of the TROY project, whose ultimate goal is to find robust evidence of exotrojan bodies and study their implications in the exoplanet field. Here, we focus on the early stages of the formation of these bodies by inspecting the iconic system PDS 70, the only confirmed planetary system in formation. Methods: We reanalyzed archival high-angular resolution Band 7 ALMA observations from PDS 70 by doing an independent imaging process to look for emission in the Lagrangian regions of the two detected gas giant protoplanets, PDS 70 b and c. We then projected the orbital paths and visually inspected emission features at the regions around the L_4/L_5 locations as defined by $\pm$ 60° in azimuth from the planet position. Results: We found emission at a $\sim$4-σ level ($\sim$6-σ when correcting from a cleaning effect) at the position of the L_5 region of PDS 70 b. This emission corresponds to a dust mass in a range of 0.03- 2 M_{Moon}, which potentially accumulated in this gravitational well. Conclusions: The tentative detection of the co-orbital dust trap that we report requires additional observations to be confirmed. We predict that we could detect the co-orbital motion of PDS 70 b and the dust presumably associated with L_5 by observing again with the same sensitivity and angular resolution as early as February 2026.

7. An imaged 15 Mjup companion within a hierarchical quadruple system

A. Chomez, V. Squicciarini, A. -M. Lagrange, P. Delorme, G. Viswanath, M. Janson, O. Flasseur, G. Chauvin, M. Langlois, P. Rubini, S. Bergeon, D. Albert, M. Bonnefoy, S. Desidera, N. Engler, R. Gratton, T. Henning, E. E. Mamajek, G. -D. Marleau, M. R. Meyer, S. Reffert, S. C. Ringqvist, M. Samland ★ Since 2019, the direct imaging B-star Exoplanet Abundance Study (BEAST) at SPHERE@VLT has been scanning the surroundings of young B-type stars in order to ascertain the ultimate frontiers of giant planet formation. Recently, the 17^{+3}_{-4} Myr HIP 81208 was found to host a close-in (50 au) brown dwarf and a wider (230 au) late M star around the central 2.6Msun primary. Alongside the continuation of the survey, we are undertaking a complete reanalysis of archival data aimed at improving detection performances so as to uncover additional low-mass companions. We present here a new reduction of the observations of HIP 81208 using PACO ASDI, a recent and powerful algorithm dedicated to processing high-contrast imaging datasets, as well as more classical algorithms and a dedicated PSF-subtraction approach. The combination of different techniques allowed for a reliable extraction of astrometric and photometric parameters. A previously undetected source was recovered at a short separation from the C component of the system. Proper motion analysis provided robust evidence for the gravitational bond of the object to HIP 81208 C. Orbiting C at a distance of 20 au, this 15Mjup brown dwarf becomes the fourth object of the hierarchical HIP 81208 system. Among the several BEAST stars which are being found to host substellar companions, HIP 81208 stands out as a particularly striking system. As the first stellar binary system with substellar companions around each component ever found by direct imaging, it yields exquisite opportunities for thorough formation and dynamical follow-up studies.

8. Composition constraints of the TRAPPIST-1 planets from their formation

Anna C. Childs, Cody Shakespeare, David R. Rice, Chao-Chin Yang, Jason H. Steffen ★ We study the formation of the TRAPPIST-1 (T1) planets starting shortly after Moon-sized bodies form just exterior to the ice line. Our model includes mass growth from pebble accretion and mergers, fragmentation, type-I migration, and eccentricity and inclination dampening from gas drag. We follow the composition evolution of the planets fed by a dust condensation code that tracks how various dust species condense out of the disc as it cools. We use the final planet compositions to calculate the resulting radii of the planets using a new planet interior structure code and explore various interior structure models. Our model reproduces the broader architecture of the T1 system and constrains the initial water mass fraction of the early embryos and the final relative abundances of the major refractory elements. We find that the inner two planets likely experienced giant impacts and fragments from collisions between planetary embryos often seed the small planets that subsequently grow through pebble accretion. Using our composition constraints we find solutions for a two-layer model, a planet comprised of only a core and mantle, that match observed bulk densities for the two inner planets b and c. This, along with the high number of giant impacts the inner planets experienced, is consistent with recent observations that these planets are likely dessicated. However, two-layer models seem unlikely for most of the remaining outer planets which suggests that these planets have a primordial hydrosphere. Our composition constraints also indicate that no planets are consistent with a core-free interior structure.

9. Radio multiwavelength analysis of the compact disk CX Tau: strong free-free variability or anomalous microwave emission?

Pietro Curone, Leonardo Testi, Enrique Macias, Marco Tazzari, Stefano Facchini, Jonathan P. Williams, Cathie J. Clarke, Antonella Natta, Giovanni Rosotti, Claudia Toci, Giuseppe Lodato ★ Protoplanetary disks emit radiation across a broad range of wavelengths, requiring a multiwavelength approach to fully understand their physical mechanisms and how they form planets. Observations at sub-millimeter to centimeter wavelengths can provide insights into the thermal emission from dust, free-free emission from ionized gas, and possible gyro-synchrotron emission from the stellar magnetosphere. This Letter focuses on CX Tau, a $\sim$0.4 $M_\odot$ star with an extended gas emission and a compact and apparently structureless dust disk, with an average millimeter flux when compared to Class II sources in Taurus. We present Karl G. Jansky Very Large Array (VLA) observations in 4 bands (between 9.0 mm and 6.0 cm) and combine them with archival data from the Atacama Large Millimeter/submillimeter Array (ALMA), the Submillimeter Array (SMA) and the Plateau de Bure Interferometer (PdBI). Such a multiwavelength approach allows to separate the dust continuum from other emissions. After isolating the dust thermal emission, we derived an upper limit of the dust disk extent at 1.3 cm which is consistent with theoretical predictions of a radial drift-dominated disk. Centimeter data show a peculiar behavior: deep observations at 6.0 cm did not detect the source, while at 1.3 cm the flux density is anomalously higher than adjacent bands. Intraband spectral indices suggest a dominant contribution from free-free emission, whereas gyro-synchrotron emission is excluded. To explain these observations, we propose strong variability of the free-free emission with timescales shorter than a month. Another possible interpretation is the presence of anomalous microwave emission from spinning dust grains.

10. DiskMINT: A Tool to Estimate Disk Masses with CO Isotopologues

Dingshan Deng, Maxime Ruaud, Uma Gorti, Ilaria Pascucci ★ CO is one of the most abundant molecules in protoplanetary disks, and optically thin emission from its isotopologues has been detected in many of them. However, several past works have argued that reproducing the relatively low emission of CO isotopologues requires a very low disk mass or significant

CO depletion. Here, we present a Python code, DiskMINT, which includes gas density and temperature structures that are both consistent with the thermal pressure gradient, isotope-selective chemistry, and conversion of CO into CO_2 ice on grain-surfaces. The code generates a self-consistent disk structure, where the gas disk distribution is obtained from a Spectral Energy Distribution (SED)-derived dust disk structure with multiple grain sizes. We use DiskMINT to study the disk of RU Lup, a high-accreting star whose disk was previously inferred to have a gas mass of only $\sim 1.5 \times 10^{-3}\,M_\odot$ and gas-to-dust mass ratio of ~ 4. Our best-fit model to the long-wavelength continuum emission can explain the total $C^{18}O$ luminosity as well as the $C^{18}O$ velocity and radial intensity profiles, and obtains a gas mass of $\sim 1.2 \times 10^{-2}\,M_\odot$, an order of magnitude higher than previous results. A disk model with parametric Gaussian vertical distribution that better matches the IR-SED can also explain the observables above with a similarly high gas mass $\sim 2.1 \times 10^{-2}\,M_\odot$. We confirm the conclusions of Ruaud et al. (2022) that optically thin $C^{18}O$ rotational lines provide reasonable estimates of the disk mass and can therefore be used as gas disk tracers.

11. Origin of Low-^{26}Al/^{27}Al Corundum/Hibonite Inclusions in Meteorites

Steven J. Desch, Emilie T. Dunham, Ashley K. Herbst, Cayman T. Unterborn, Thomas G. Sharp, Maitrayee Bose, Prajkta Mane, Curtis D. Williams ★ Most meteoritic calcium-rich, aluminum-rich inclusions (CAIs) formed from a reservoir with $^{26}Al/^{27}Al \approx 5 \times 10^{-5}$, but some record lower $(^{26}Al/^{27}Al)_0$, demanding they sampled a reservoir without live ^{26}Al. This has been interpreted as evidence for "late injection" of supernova material into our protoplanetary disk. We instead interpret the heterogeneity as chemical, demonstrating that these inclusions are strongly associated with the refractory phases corundum or hibonite. We name them "Low-^{26}Al/^{27}Al Corundum/Hibonite Inclusions" (LAACHIs). We present a detailed astrophysical model for LAACHI formation in which they derive their Al from presolar corundum, spinel or hibonite grains $0.5-2\,\mu$m in size with no live ^{26}Al; live ^{26}Al is carried on smaller (<50 nm) presolar chromium spinel grains from recent nearby Wolf-Rayet stars or supernovae. In hot ($\approx$ 1350-1425 K) regions of the disk these grains, and perovskite grains, would be the only survivors. These negatively charged grains would grow to sizes $1-10^3\,\mu$m, even incorporating positively charged perovskite grains, but not the small, negatively charged ^{26}Al-bearing grains. Chemical and isotopic fractionations due to grain charging was a significant process in hot regions of the disk. Our model explains the sizes, compositions, oxygen isotopic signatures, and the large, correlated ^{48}Ca and ^{50}Ti anomalies (if carried by presolar perovskite) of LAACHIs, and especially how they incorporated no ^{26}Al in a solar nebula with uniform, canonical ^{26}Al/^{27}Al. A late injection of supernova material is obviated, although formation of the Sun in a high-mass star-forming region is demanded.

12. Azimuthal patterns in planetesimal circumstellar disks

Tatiana V. Demidova, Ivan I. Shevchenko ★ Ways of formation of azimuthal resonant patterns in circumstellar planetesimal disks with planets are considered. Our analytical estimates and massive numerical experiments show that the disk particles that initially reside in zones of low-order mean-motion resonances with the planet may eventually concentrate into potentially observable azimuthal patterns. The structuring process is rapid, usually taking 100 orbital periods of the planet. It is found that the relative number of particles that retain their resonant position increases with decreasing the mass parameter μ (the ratio of masses of the perturbing planet and the parent star), but a significant fraction of the particle population is always removed from the disk due to accretion of the particles onto the star and planet, as well as due to their transition to highly elongated and hyperbolic orbits. Expected radio images of azimuthally structured disks are constructed. In the considered models, azimuthal patterns associated with the 2:1 and 3:2 resonances are most clearly manifested; observational manifestations of the 1:2 and 2:3 resonances are also possible.

13. The sharpest view on the high-mass star-forming region S255IR. Near-InfraRed Adaptive Optics Imaging on the Outbursting Source NIRS3

R. Fedriani, A. Caratti o Garatti, R. Cesaroni, J. C. Tan, B. Stecklum, L. Moscadelli, M. Koutoulaki, G. Cosentino, M. Whittle ★ Massive stars have an impact on their surroundings from early in their formation until the end of their lives. However, very little is known about their formation. Episodic accretion may play a crucial role, but observations of these events have only been reported towards a handful of massive protostars. We aim to investigate the outburst event from the high-mass star-forming region S255IR where recently the protostar NIRS3 underwent an accretion outburst. We follow the evolution of this source both in photometry and morphology of its surroundings. Methods: We perform near-infrared adaptive optics observations on the S255IR central region using the Large Binocular Telescope in the K_s broad-band and the H_2 and Brγ narrow-band filters with an angular resolution of ~ 0.06 arcsec, close to the diffraction limit. We discover a new near-infrared knot north-east from NIRS3 that we interpret as a jet knot that was ejected during the last accretion outburst and observed in the radio regime as part of a follow-up after the outburst. We measure a mean tangential velocity for this knot of $450 \pm 50\,\mathrm{km\,s^{-1}}$. We analyse the continuum-subtracted images from H_2 which traces jet shocked emission, and Brγ which traces scattered light from a combination of accretion activity and UV radiation from the central massive protostar. We observe a significant decrease in flux at the location of NIRS3, with K=13.48 mag being the absolute minimum in the historic series. Our observations strongly suggest a scenario where the episodic accretion is followed by an episodic ejection response in the near-infrared, as it was seen in the earlier radio follow-up. The 30 years of $\sim 2\,\mu$m photometry suggests that NIRS3

might have undergone another outburst in the late 1980s, being the first massive protostar with such evidence observed in the near-infrared.

14. The Radial Distribution and Excitation of H2 around Young Stars in the HST-ULLYSES Survey

Kevin France, Nicole Arulanantham, Erin Maloney, P. Wilson Cauley, P. Abraham, Juan M. Alcala, Justyn Campbell-White, Eleonora Fiorellino, Gregory J. Herczeg, Brunella Nisini, Miguel Vioque ★ The spatial distribution and evolution of gas in the inner 10 au of protoplanetary disks form the basis for estimating the initial conditions of planet formation. Among the most important constraints derived from spectroscopic observations of the inner disk are the radial distributions of the major gas phase constituents, how the properties of the gas change with inner disk dust evolution, and how chemical abundances and excitation conditions are influenced by the high-energy radiation from the central star. We present a survey of the radial distribution, excitation, and evolution of inner disk molecular hydrogen (H_2) obtained as part of the *HST*/ULLYSES program. We analyze far-ultraviolet spectroscopy of 71 (63 accreting) pre-main sequence systems in the ULLYSES DR5 release to characterize the H_2 emission lines, H_2 dissociation continuum emission, and major photochemical/disk evolution driving UV emissions (Lyα, UV continuum, and C IV). We use the widths of the H_2 emission lines to show that most fluorescent H_2 arises between 0.1 - 1.4 au from the parent star, and show positive correlations of the average emitting radius with the accretion luminosity and with the dust disk mass. We find a strong correlation between H_2 dissociation emission and both the accretion-dominated Lyα luminosity and the inner disk dust clearing, painting a picture where water molecules in the inner 3 au are exposed to and dissociated by strong Lyα emission as the opacity of the inner disk declines with time.

15. Disk and Envelope Streamers of the GGD27-MM1 Massive Protostar

M. Fernández-López, J. M. Girart, J. A. López-Vázquez, R. Estalella, G. Busquet, S. Curiel, N. Añez-López ★ We present new Atacama Large (sub)Millimeter Array 0.98 mm observations of the continuum emission and several molecular lines toward the high-mass protostellar system GGD27-MM1, driving the HH 80-81 radio-jet. The detailed analysis of the continuum and the CH_3CN molecular emission allows us to separate the contributions from the dust content of the disk (extending up to 190 au), the molecular content of the disk (extending from 140 to 360 au), and the content of the envelope, revealing the presence of several possible accretion streamers (also seen in other molecular tracers, such as CH_3OH). We analyze the physical properties of the system, producing temperature and column density maps, and radial profiles for the disk and the envelope. We qualitatively reproduce the trajectories and line-of-sight velocities of the possible streamers using a theoretical model approach. An ad-hoc model of a flared disk comprising a hot dust disk embedded in cold gas fits the H_2S emission, which revealed the molecular disk as crescent-shape with a prominent central absorption. Another fit to the central absorption spectrum suggests that the absorption is probably caused by different external cold layers from the envelope or the accretion streamers. Finally, the analysis of the rotation pattern of the different molecular transitions in the molecular disk, suggests that there is an inner zone devoid of molecular content.

16. A high-resolution radio study of the L1551 IRS 5 and L1551 NE jets

A. Feeney-Johansson, S. J. D. Purser, T. P. Ray, C. Carrasco-González, A. Rodríguez-Kamenetzky, J. Eislöffel, J. Lim, R. Galván-Madrid, S. Lizano, L. F. Rodríguez, H. Shang, P. Ho, M. Hoare ★ Using observations with e-MERLIN and the VLA, together with archival data from ALMA, we obtain high-resolution radio images of two binary YSOs: L1551 IRS 5 and L1551 NE, covering a wide range of frequencies from 5 - 336 GHz, and resolving emission from the radio jet on scales of only 15 au. By comparing these observations to those from a previous epoch, it is shown that there is a high degree of variability in the free-free emission from the jets of these sources. In particular, the northern component of L1551 IRS 5 shows a remarkable decline in flux density of a factor of 5, suggesting that the free-free emission of this source has almost disappeared. By fitting the spectra of the sources, the ionised mass-loss rates of the jets are derived and it is shown that there is significant variability of up to a factor of 6 on timescales of 20 years. Using radiative transfer modelling, we also obtained a model image for the jet of the southern component of L1551 IRS 5 to help study the inner region of the ionised high-density jet. The findings favour the X-wind model launched from a very small innermost region.

17. Unravelling the structure of magnetised molecular clouds with SILCC-Zoom: sheets, filaments and fragmentation

S. Ganguly, S. Walch, D. Seifried, S. D. Clarke, M. Weis ★ To what extent magnetic fields affect how molecular clouds (MCs) fragment and create dense structures is an open question. We present a numerical study of cloud fragmentation using the SILCC-Zoom simulations. These simulations follow the self-consistent formation of MCs in a few hundred parsec sized region of a stratified galactic disc; and include magnetic fields, self-gravity, supernova-driven turbulence, as well as a non-equilibrium chemical network. To discern the role of magnetic fields in the evolution of MCs, we study seven simulated clouds, five with magnetic fields, and two without, with a maximum resolution of 0.1 parsec. Using a dendrogram we identify hierarchical

structures which form within the clouds. Overall, the magnetised clouds have more mass in a diffuse envelope with a number density between 1-100 cm^{-3}. We find that six out of seven clouds are sheet-like on the largest scales, as also found in recent observations, and with filamentary structures embedded within, consistent with the bubble-driven MC formation mechanism. Hydrodynamic simulations tend to produce more sheet-like structures also on smaller scales, while the presence of magnetic fields promotes filament formation. Analysing cloud energetics, we find that magnetic fields are dynamically important for less dense, mostly but not exclusively atomic structures (typically up to $\sim 100 - 1000$ cm^{-3}), while the denser, potentially star-forming structures are energetically dominated by self-gravity and turbulence. In addition, we compute the magnetic surface term and demonstrate that it is generally confining, and some atomic structures are even magnetically held together. In general, magnetic fields delay the cloud evolution and fragmentation by ~ 1 Myr.

18. **Early Planet Formation in Embedded Disks (eDisk) III: A first high-resolution view of sub-mm continuum and molecular line emission toward the Class 0 protostar L1527 IRS**

Merel L. R. van 't Hoff, John J. Tobin, Zhi-Yun Li, Nagayoshi Ohashi, Jes K. Jørgensen, Zhe-Yu Daniel Lin, Yuri Aikawa, Yusuke Aso, Itziar de Gregorio-Monsalvo, Sacha Gavino, Ilseung Han, Patrick M. Koch, Woojin Kwon, Chang Won Lee, Jeong-Eun Lee, Leslie W. Looney, Suchitra Narayanan, Adele Plunkett, Jinshi Sai, Alejandro Santamaría-Miranda, Rajeeb Sharma, Patrick D. Sheehan, Shigehisa Takakuwa, Travis J. Thieme, Jonathan P. Williams, Shih-Ping Lai, Nguyen Thi Phuong, Hsi-Wei Yen ★ Studying the physical and chemical conditions of young embedded disks is crucial to constrain the initial conditions for planet formation. Here, we present Atacama Large Millimeter/submillimeter Array (ALMA) observations of dust continuum at ∼0.06" (8 au) resolution and molecular line emission at ∼0.17" (24 au) resolution toward the Class 0 protostar L1527 IRS from the Large Program eDisk (Early Planet Formation in Embedded Disks). The continuum emission is smooth without substructures, but asymmetric along both the major and minor axes of the disk as previously observed. The detected lines of ^{12}CO, ^{13}CO, $C^{18}O$, H_2CO, c-C_3H_2, SO, SiO, and DCN trace different components of the protostellar system, with a disk wind potentially visible in ^{12}CO. The ^{13}CO brightness temperature and the H_2CO line ratio confirm that the disk is too warm for CO freeze out, with the snowline located at ∼350 au in the envelope. Both molecules show potential evidence of a temperature increase around the disk-envelope interface. SO seems to originate predominantly in UV-irradiated regions such as the disk surface and the outflow cavity walls rather than at the disk-envelope interface as previously suggested. Finally, the continuum asymmetry along the minor axis is consistent with the inclination derived from the large-scale (100" or 14,000 au) outflow, but opposite to that based on the molecular jet and envelope emission, suggesting a misalignment in the system. Overall, these results highlight the importance of observing multiple molecular species in multiple transitions to characterize the physical and chemical environment of young disks.

19. **How does accretion of planet-forming disks influence stellar abundances?**

León-Alexander Hühn, Bertram Bitsch ★ Millimeter sized dust grains experience radial velocities exceeding the gas velocities by orders of magnitude. The viscous evolution of the accretion disk adds disk material onto the central star's convective envelope, influencing its elemental abundances, [X/H]. At the same time, the envelope mass shrinks over time, amplifying the rate of abundance change. Therefore, the elemental abundances of the star are sensitive to disk processes that alter the composition and timing of disk accretion. We perform numerical 1D log-radial simulations integrating the disk advection-diffusion equation, accounting for phase transitions of chemical species at the evaporation fronts. They reveal a peak of refractory abundance within the first 2 Myr of Δ[X/H] $\sim 5 \times 10^{-2}$ if grain growth is significant, but subsequent accretion diminishes previous refractory abundance increases for long-lived disks. Planet formation can reduce the abundance of dust species whose evaporation fronts lie within the planet's orbit by opening a gap and consequently blocking inward drifting pebbles. We expect the accretion of the Solar protoplanetary disk with Jupiter present to have changed the Sun's elemental abundances by $\sim 10^{-2}$ throughout its lifetime. These considerations are also applied to the HD106515 wide binary system. We find that measurements of Δ[X/H] are in reasonable agreement with results from simulations where the observed giant planet around HD106515 A is included and if HD106515B's disk formed planetesimals more efficiently. Simulations where the planet formed inside the water ice line are more favorable to agree with observations. Even though the general changes in the stellar abundances due to disk accretion are small, they are detectable at current sensitivities, indicating that the here presented methods can be used to constrain the planet formation pathway.

20. **The extremely sharp transition between molecular and ionized gas in the Horsehead nebula**

C. Hernández-Vera, V. V. Guzmán, J. R. Goicoechea, V. Maillard, J. Pety, F. Le Petit, M. Gerin, E. Bron, E. Roueff, A. Abergel, T. Schirmer, J. Carpenter, P. Gratier, K. Gordon, K. Misselt ★ (Abridged) Massive stars can determine the evolution of molecular clouds with their strong ultraviolet (UV) radiation fields. Moreover, UV radiation is relevant in setting the thermal gas pressure in star-forming clouds, whose influence can extend from the rims of molecular clouds to entire star-forming galaxies. Probing the fundamental structure of nearby molecular clouds is therefore crucial to understand how massive stars shape their surrounding medium and how fast molecular clouds are destroyed, specifically at

their UV-illuminated edges, where models predict an intermediate zone of neutral atomic gas between the molecular cloud and the surrounding ionized gas whose size is directly related to the exposed physical conditions. We present the highest angular resolution (0.5", corresponding to 207 au) and velocity-resolved images of the molecular gas emission in the Horsehead nebula, using CO J=3-2 and HCO^+ J=4-3 observations with ALMA. We find that CO and HCO^+ are present at the edge of the cloud, very close to the ionization (H^+/H) and dissociation fronts (H/H_2), suggesting a very thin layer of neutral atomic gas (<650 au) and a small amount of CO-dark gas ($A_V = 0.006 - 0.26$ mag) for stellar UV illumination conditions typical of molecular clouds in the Milky Way. The new ALMA observations reveal a web of molecular gas filaments with an estimated thermal gas pressure of $P_{\rm th} = (2.3 - 4.0) \times 10^6$ K cm^{-3}, and the presence of a steep density gradient at the cloud edge that can be well explained by stationary isobaric PDR models with pressures consistent with our estimations. However, in the HII region and PDR interface, we find $P_{\rm th,PDR} > P_{\rm th,HII}$, suggesting the gas is slightly compressed. Therefore, dynamical effects cannot be completely ruled out and even higher angular observations will be needed to unveil their role.

21. Mapping gravity in stellar nurseries – establishing the effectiveness of 2D acceleration maps

Zhen-Zhen He, Guang-Xing Li, Andreas Burkert ★ Gravity is the driving force of star formation. Although gravity is caused by the presence of matter, its role in complex regions is still unsettled. One effective way to study the pattern of gravity is to compute the accretion it exerts on the gas by providing gravitational acceleration maps. A practical way to study acceleration is by computing it using 2D surface density maps, yet whether these maps are accurate remains uncertain. Using numerical simulations, we confirm that the accuracy of the acceleration maps $\mathbf{a}_{\rm 2D}(x, y)$ computed from 2D surface density are good representations for the mean acceleration weighted by mass. Due to the under-estimations of the distances from projected maps, the magnitudes of accelerations will be over-estimated $|\mathbf{a}_{\rm 2D}(x, y)| \approx 2.3 \pm 1.8\ |\mathbf{a}^{\rm proj}_{\rm 3D}(x, y)|$, where $\mathbf{a}^{\rm proj}_{\rm 3D}(x, y)$ is mass-weighted projected gravitational acceleration, yet $\mathbf{a}_{\rm 2D}(x, y)$ and $\mathbf{a}^{\rm proj}_{\rm 3D}(x, y)$ stay aligned within 20°. Significant deviations only occur in regions where multiple structures are present along the line of sight. The acceleration maps estimated from surface density provide good descriptions of the projection of 3D acceleration fields. We expect this technique useful in establishing the link between cloud morphology and star formation, and in understanding the link between gravity and other processes such as the magnetic field. A version of the code for calculating surface density gravitational potential is available at `https://github.com/zhenzhen-research/phi_2d`.

22. Investigation of the rotational spectrum of CD_3OD and an astronomical search toward IRAS 16293−2422

V. V. Ilyushin, H. S. P. Müller, J. K. Jørgensen, S. Bauerecker, C. Maul, R. Porohovoi, E. A. Alekseev, O. Dorovskaya, F. Lewen, S. Schlemmer, R. M. Lees ★ Solar-type prestellar cores and protostars display large amounts of deuterated organic molecules. Recent findings on CHD_2OH and CD_3OH toward IRAS 16293-2422 suggest that even fully deuterated methanol, CD_3OD, may be detectable as well. However, searches for CD_3OD are hampered in particular by the lack of intensity information from a spectroscopic model. The objective of the present investigation is to develop a spectroscopic model of CD_3OD in low-lying torsional states that is sufficiently accurate to facilitate searches for this isotopolog in space. We carried out a new measurement campaign for CD_3OD involving two spectroscopic laboratories that covers the 34 GHz-1.1 THz range. A torsion-rotation Hamiltonian model based on the rho-axis method was employed for our analysis. Our resulting model describes the ground and first excited torsional states of CD_3OD well up to quantum numbers $J \leq 51$ and $K_a \leq 23$. We derived a line list for radio-astronomical observations from this model that is accurate up to at least 1.1 THz and should be sufficient for all types of radio-astronomical searches for this methanol isotopolog. This line list was used to search for CD_3OD in data from the Protostellar Interferometric Line Survey of IRAS 16293−2422 obtained with the Atacama Large Millimeter/submillimeter Array. While we found several emission features that can be attributed largely to CD_3OD, their number is still not sufficiently high enough to establish a clear detection. Nevertheless, the estimate of 2×10^{15} cm^{-2} derived for the CD_3OD column density may be viewed as an upper limit that can be compared to column densities of CD_3OH, CH_3OD, and CH_3OH. The comparison indicates that the CD_3OD column density toward IRAS 16293-2422 is in line with the enhanced D/H ratios observed for multiply deuterated complex organic molecules.

23. Chemical footprints of giant planet formation. Role of planet accretion in shaping the C/O ratio of protoplanetary disks

Haochang Jiang, Yu Wang, Chris W. Ormel, Sebastiaan Krijt, Ruobing Dong ★ Protoplanetary disks, the birthplaces of planets, commonly feature bright rings and dark gaps in both continuum and line emission maps. Accreting planets are interacting with the disk, not only through gravity, but also by changing the local irradiation and elemental abundances, which are essential ingredients for disk chemistry. We propose that giant planet accretion can leave chemical footprints in the gas local to the planet, which potentially leads to the spatial coincidence of molecular emissions with the planet in ALMA observation. Through 2D multi-fluid hydrodynamical simulations in Athena++ with built-in sublimation, we simulate the process of an accreting planet locally heating up its vicinity, opening a gas gap in the disk, and creating the conditions for C-photochemistry.

An accreting planet located outside the methane snowline can render the surrounding gas hot enough to sublimate the C-rich organics off pebbles before they are accreted by the planet. This locally elevates the disk gas-phase C/O ratio, providing a potential explanation for the C_2H line-emission rings observed with ALMA. In particular, our findings provide an explanation for the MWC480 disk, where previous work has identified a statistically significant spatial coincidence of line-emission rings inside a continuum gap. Our findings present a novel view of linking the gas accretion of giant planets and their natal disks through the chemistry signals. This model demonstrates that giant planets can actively shape their forming chemical environment, moving beyond the traditional understanding of the direct mapping of primordial disk chemistry onto planets.

24. Early Planet Formation in Embedded Disks (eDisk). VII. Keplerian Disk, Disk Substructure, and Accretion Streamers in the Class 0 Protostar IRAS 16544-1604 in CB 68

Miyu Kido, Shigehisa Takakuwa, Kazuya Saigo, Nagayoshi Ohashi, John J. Tobin, Jes K, Jørgensen, Yuri Aikawa, Yusuke Aso, Frankie J. Encalada, Christian Flores, Sacha Gavino, Itziar de Gregorio-Monsalvo, Ilseung Han, Shingo Hirano, Patrick M. Koch, Woojin Kwon, Shih-Ping Lai, Chang Won Lee, Jeong-Eun Lee, Zhi-Yun Li, Zhe-Yu Daniel Lin, Leslie W. Looney, Shoji Mori, Suchitra Narayanan, Adele L. Plunkett, Nguyen Thi Phuong, Jinshi Sai, Alejandro Santamarîa-Miranda, Rajeeb Sharma, Patrick Sheehan, Travis J. Thieme, Kengo Tomida, Merel L. R. van't Hoff, Jonathan P. Williams, Yoshihide Yamato, Hsi-Wei Yen ★ We present observations of the Class 0 protostar IRAS 16544-1604 in CB 68 from the "Early Planet Formation in Embedded Disks (eDisk)" ALMA Large program. The ALMA observations target continuum and lines at 1.3-mm with an angular resolution of ∼5 au. The continuum image reveals a dusty protostellar disk with a radius of ∼30 au seen close to edge-on, and asymmetric structures both along the major and minor axes. While the asymmetry along the minor axis can be interpreted as the effect of the dust flaring, the asymmetry along the major axis comes from a real non-axisymmetric structure. The $C^{18}O$ image cubes clearly show the gas in the disk that follows a Keplerian rotation pattern around a ∼0.14 $M_\odot$ central protostar. Furthermore, there are ∼1500 au-scale streamer-like features of gas connecting from North-East, North-North-West, and North-West to the disk, as well as the bending outflow as seen in the ^{12}CO (2-1) emission. At the apparent landing point of NE streamer, there are SO (6_5-5_4) and SiO (5-4) emission detected. The spatial and velocity structure of NE streamer can be interpreted as a free-falling gas with a conserved specific angular momentum, and the detection of the SO and SiO emission at the tip of the streamer implies presence of accretion shocks. Our eDisk observations have unveiled that the Class 0 protostar in CB 68 has a Keplerian rotating disk with flaring and non-axisymmetric structure associated with accretion streamers and outflows.

25. Metallicity Dependence of Molecular Cloud Hierarchical Structure at Early Evolutionary Stages

Masato I. N. Kobayashi, Kazunari Iwasaki, Kengo Tomida, Tsuyoshi Inoue, Kazuyuki Omukai, Kazuki Tokuda ★ The formation of molecular clouds out of HI gas is the first step toward star formation. Its metallicity dependence plays a key role to determine star formation through the cosmic history. Previous theoretical studies with detailed chemical networks calculate thermal equilibrium states and/or thermal evolution under one-zone collapsing background. The molecular cloud formation in reality, however, involves supersonic flows, and thus resolving the cloud internal turbulence/density structure in three dimension is still essential. We here perform magnetohydrodynamics simulations of 20 km/s converging flows of Warm Neutral Medium (WNM) with 1 micro Gauss mean magnetic field in the metallicity range from the Solar (1.0 Zsun) to 0.2 Zsun environment. The Cold Neutral Medium (CNM) clumps form faster with higher metallicity due to more efficient cooling. Meanwhile, their mass functions commonly follow dn/dm proportional to $m^{-1.7}$ at three cooling times regardless of the metallicity. Their total turbulence power also commonly shows the Kolmogorov spectrum with its 80 percent in the solenoidal mode, while the CNM volume alone indicates the transition towards the Larson's law. These similarities measured at the same time in the unit of the cooling time suggest that the molecular cloud formation directly from the WNM alone requires a longer physical time in a lower metallicity environment in the 1.0–0.2 Zsun range. To explain the rapid formation of molecular clouds and subsequent massive star formation possibly within less than 10 Myr as observed in the Large/Small Magellanic Clouds (LMC/SMC), the HI gas already contains CNM volume instead of pure WNM.

26. The Effect of Dust Evolution and Traps on Inner Disk Water Enrichment

Anusha Kalyaan, Paola Pinilla, Sebastiaan Krijt, Andrea Banzatti, Giovanni Rosotti, Gijs D. Mulders, Michiel Lambrechts, Feng Long, Gregory J. Herczeg ★ Substructures in protoplanetary disks can act as dust traps that shape the radial distribution of pebbles. By blocking the passage of pebbles, the presence of gaps in disks may have a profound effect on pebble delivery into the inner disk, crucial for the formation of inner planets via pebble accretion. This process can also affect the delivery of volatiles (such as H_2O) and their abundance within the water snow line region (within a few au). In this study, we aim to understand what effect the presence of gaps in the outer gas disk may have on water vapor enrichment in the inner disk. Building on previous work, we employ a volatile-inclusive multi-Myr disk evolution model that considers an evolving ice-bearing drifting dust population, sensitive to dust-traps, which loses its icy content to sublimation upon reaching the snow line. We find that vapor abundance in the inner disk is strongly affected by fragmentation velocity (v_f) and turbulence,

which control how intense vapor enrichment from pebble delivery is, if present, and how long it may last. Generally, for disks with low to moderate turbulence ($\alpha \leq 1 \times 10^{-3}$) and for a range of v_f, radial location, and gap depth (especially that of the innermost gaps), can significantly alter enrichment. Shallow inner gaps may continuously leak material from beyond it, despite the presence of additional deep outer gaps. We finally find that the for realistic v_f (≤ 10 m s^{-1}), presence of gaps is more important than planetesimal formation beyond the snow line in regulating pebble and volatile delivery into the inner disk.

27. Giant Impact Events for Protoplanets: Energetics of Atmospheric Erosion by Head-on Collision

Kenji Kurosaki, Shu-ichiro Inutsuka ★ Numerous exoplanets with masses ranging from Earth to Neptune and radii larger than Earth have been found through observations. These planets possess atmospheres that range in mass fractions from 1% to 30%, reflecting the diversity of atmospheric mass fractions. Such diversities are supposed to be caused by differences in the formation processes or evolution. Here we consider head-on giant impacts onto planets causing atmosphere losses in the later stage of their formation. We perform smoothed particle hydrodynamic simulations to study the impact-induced atmosphere loss of young super-Earths with 10%-30% initial atmospheric mass fractions. We find that the kinetic energy of the escaping atmosphere is almost proportional to the sum of the kinetic impact energy and self-gravitational energy released from the merged core. We derive the relationship between the kinetic impact energy and the escaping atmosphere mass. The giant impact events for planets of comparable masses are required in the final stage of the popular scenario of rocky planet formation. We show it results in a significant loss of the atmosphere, if the impact is a head-on collision with comparable masses. This latter fact provides a constraint on the formation scenario of rocky planets with substantial atmospheres.

28. Ro-vibrational Spectroscopy of CI Tau – Evidence of a Multi-Component Eccentric Disk Induced by a Planet

Janus Kozdon, Sean Brittain, Jeffrey Fung, Josh Kern, Stanley Jensen, John Carr, Joan Najita, Andrea Banzatti ★ CI Tau is currently the only T Tauri star with an inner protoplanetary disk that hosts a planet, CI Tau b, that has been detected by a radial velocity survey. This provides the unique opportunity to study disk features that were imprinted by that planet. We present multi-epoch spectroscopic data, taken with NASA IRTF in 2022, of the ^{12}CO and hydrogen Pfβ line emissions spanning 9 consecutive nights, which is the proposed orbital period of CI Tau b. We find that the star's accretion rate varied according to that 9 d period, indicative of companion driven accretion. Analysis of the ^{12}CO emission lines reveals that the disk can be described with an inner and outer component spanning orbital radii 0.05-0.13 au and 0.15-1.5 au, respectively. Both components have eccentricities of about 0.05 and arguments of periapses that are oppositely aligned. We present a proof-of-concept hydrodynamic simulation that shows a massive companion on a similarly eccentric orbit can recreate a similar disk structure. Our results allude to such a companion being located around an orbital distance of 0.14 au. However, this planet's orbital parameters may be inconsistent with those of CI Tau b whose high eccentricity is likely not compatible with the low disk eccentricities inferred by our model.

29. Rapid Formation of Gas-giant Planets via Collisional Coagulation from Dust Grains to Planetary Cores. II. Dependence on Pebble Bulk Density and Disk Temperature

Hiroshi Kobayashi, Hidekazu Tanaka ★ Thanks to "dust-to-planet" simulations (DTPSs), which treat the collisional evolution directly from dust to giant-planet cores in a protoplanetary disk, we showed that giant-planet cores are formed in $\lesssim 10$ au in several 10^5 years, because porous pebbles grow into planetesimals via collisions prior to drift in 10 au (Kobayashi & Tanaka 2021, Paper I).However, such porous pebbles are unlikely to reproduce the polarized millimeter wavelength light observed from protoplanetary disks. We thus investigate gas-giant core formation with non-porous pebbles via DTPSs. Even non-porous bodies can grow into planetesimals and massive cores to be gas giants are also formed in several 10^5 years. The rapid core formation is mainly via the accretion of planetesimals produced by collisional coagulation of pebbles drifting from the outer disk. The formation mechanism is similar to the case with porous pebbles, while core formation occurs in a wider region (5 - 10 au) than that with porous pebbles.

30. Early Planet Formation in Embedded Disks (eDisk). II. Limited Dust Settling and Prominent Snow Surfaces in the Edge-on Class I Disk IRAS 04302+2247

Zhe-Yu Daniel Lin, Zhi-Yun Li, John J. Tobin, Nagayoshi Ohashi, Jes Kristian Jørgensen, Leslie W. Looney, Yusuke Aso, Shigehisa Takakuwa, Yuri Aikawa, Merel L. R. van 't Hoff, Itziar de Gregorio-Monsalvo, Frankie J. Encalada, Christian Flores, Sacha Gavino, Ilseung Han, Miyu Kido, Patrick M. Koch, Woojin Kwon, Shih-Ping Lai, Chang Won Lee, Jeong-Eun Lee, Nguyen Thi Phuong, Jinshi Sai, Rajeeb Sharma, Patrick Sheehan, Travis J. Thieme, Jonathan P. Williams, Yoshihide Yamato, Hsi-Wei Yen ★ While dust disks around optically visible, Class II protostars are found to be vertically thin, when and how dust settles to the midplane are unclear. As part of the Atacama Large Millimeter/submillimeter Array (ALMA) large program, Early Planet Formation in Embedded Disks, we analyze the

edge-on, embedded, Class I protostar IRAS 04302+2247, also nicknamed the “Butterfly Star." With a resolution of 0.05" (8 au), the 1.3 mm continuum shows an asymmetry along the minor axis which is evidence of an optically thick and geometrically thick disk viewed nearly edge-on. There is no evidence of rings and gaps, which could be due to the lack of radial substructure or the highly inclined and optically thick view. With 0.1" (16 au) resolution, we resolve the 2D snow surfaces, i.e., the boundary region between freeze-out and sublimation, for ^{12}CO J=2–1, ^{13}CO J=2–1, C^{18}O J=2–1, H_2CO J=$3_{0,3}$–$2_{0,2}$, and SO J=6_5–5_4, and constrain the CO midplane snow line to $\sim$ 130 au. We find Keplerian rotation around a protostar of $1.6 \pm 0.4 M_\odot$ using C^{18}O. Through forward ray-tracing using RADMC-3D, we find that the dust scale height is $\sim$ 6 au at a radius of 100 au from the central star and is comparable to the gas pressure scale height. The results suggest that the dust of this Class I source has yet to vertically settle significantly.

31. Complex Organic Molecules in a Very Young Hot Corino, HOPS 373SW

Jeong-Eun Lee, Giseon Baek, Seokho Lee, Jae-Hong Jeong, Chul-Hwan Kim, Yuri Aikawa, Gregory J. Herczeg, Doug Johnstone, John J. Tobin ★ We present the spectra of Complex Organic Molecules (COMs) detected in HOPS 373SW with the Atacama Large Millimeter/submillimeter Array (ALMA). HOPS 373SW, which is a component of a protostellar binary with a separation of 1500 au, has been discovered as a variable protostar by the JCMT Transient monitoring survey with a modest 30% brightness increase at submillimeter wavelengths. Our ALMA Target of Opportunity (ToO) observation at 345 GHz for HOPS 373SW revealed extremely young chemical characteristics with strong deuteration of methanol. The dust continuum opacity is very high toward the source center, obscuring line emission from within 0.03 arcsec. The other binary component, HOPS 373NE, was detected only in C17O in our observation, implying a cold and quiescent environment. We compare the COMs abundances relative to CH3OH in HOPS 373SW with those of V883 Ori, which is an eruptive disk object, as well as other hot corinos, to demonstrate the chemical evolution from envelope to disk. High abundances of singly, doubly, and triply deuterated methanol (CH2DOH, CHD2OH, and CD3OH) and a low CH3CN abundance in HOPS 373SW compared to other hot corinos suggest a very early evolutionary stage of HOPS 373SW in the hot corino phase. Since the COMs detected in HOPS 373SW would have been sublimated very recently from grain surfaces, HOPS 373SW is a promising place to study the surface chemistry of COMs in the cold prestellar phase, before sublimation.

32. The kinematics of young stellar population in the W5 region of the Cassiopeia OB6 association: implication on the formation process of stellar associations

Beomdu Lim, Jongsuk Hong, Jinhee Lee, Hyeong-Sik Yun, Narae Hwang, Byeong-Gon Park ★ The star-forming region W5 is a major part of the Cassiopeia OB6 association. Its internal structure and kinematics may provide hints of the star formation process in this region. Here, we present a kinematic study of young stars in W5 using the Gaia data and our radial velocity data. A total 490 out of 2,000 young stars are confirmed as members. Their spatial distribution shows that W5 is highly substructured. We identify a total of eight groups using the k-means clustering algorithm. There are three dense groups in the cavities of H II bubbles, and the other five sparse groups are distributed at the ridge of the bubbles. The three dense groups have almost the same ages (5 Myr) and show a pattern of expansion. The scale of their expansion is not large enough to account for the overall structure of W5. The three northern groups are, in fact, 3 Myr younger than the dense groups, which indicates the independent star formation events. Only one group of them shows the signature of feedback-driven star formation as its members move away from the eastern dense group. The other two groups might have formed in a spontaneous way. On the other hand, the properties of two southern groups are not understood as those of a coeval population. Their origins can be explained by dynamical ejection of stars and multiple star formation. Our results suggest that the substructures in W5 formed through multiple star-forming events in a giant molecular cloud.

33. Mass-accretion, spectral, and photometric properties of T Tauri stars in Taurus based on TESS and LAMOST

Chia-Lung Lin, Wing-Huen Ip, Yao Hsiao, Tzu-Hueng Chang, Yi-han Song, A-Li Luo ★ We present the analysis of 16 classical T Taur stars using LAMOST and TESS data, investigating spectral properties, photometric variations, and mass-accretion rates. All 16 stars exhibit emissions in Hα lines, from which the average mass-accretion rate of 1.76×10^{-9} $M_\odot yr^{-1}$ is derived. Two of the stars, DL Tau and Haro 6-13, show mass-accretion bursts simultaneously in TESS, ASAS-SN, and/or ZTF survey. Based on these observations, we find that the mass-accretion rates of DL Tau and Haro 6-13 reach their maximums of 2.5×10^{-8} $M_\odot yr^{-1}$ and 2×10^{-10} $M_\odot yr^{-1}$ during the TESS observation, respectively. We detect thirteen flares among these stars. The flare frequency distribution shows that the CTTSs' flare activity is not only dominated by strong flares with high energy but much more active than those of solar-type and young low-mass stars. By comparing the variability classes reported in the literature, we find that the transition timescale between different classes of variability in CTTSs, such as from Stochastic (S) to Bursting (B) or from quasi-periodic symmetric (QPS) to quasi-periodic dipping (QPD), may range from 1.6 to 4 years. We observe no significant correlation between inclination and mass-accretion rates derived from the emission indicators. This suggests that inner disk properties may be more important than that of outer disk. Finally, we find a relatively significant positive correlation between the asymmetric metric "M" and the cold disk inclination compared to the literature. A weak

negative correlation between the periodicity metric "Q" value and inclination has been also found.

34. Light and colour of cirrus, translucent and opaque dust in the high-latitude area of LDN 1642

K. Mattila, P. Väisänen, K. Lehtinen, L. Haikala, M. Haas ★ We have performed a 5-colour surface photometric study of the high-galactic-latitude area of dark nebula LDN 1642. Scattered light properties are presented of diffuse, translucent and opaque dust over the range of 3500 – 5500 A. Far infrared absolute photometry at 200 um improves the precision of and provides a zero point to the extinction. The intensity of the scattered light depends on dust column density in a characteristic way: for optically thin dust the intensity first increases linearly, then turns to a saturation value; at still larger extinctions the intensity turns down to a slow decrease. The A_V value of the saturated intensity maximum shifts in a systematic way, from $A_V \approx 1.5$ mag at 3500 A, to ~ 3 mag at 5500 A. The intensity curves offer a straight-forward explanation for the behaviour of the scattered-light colours. At the intensity peak the colour agrees with the integrated starlight colour, while it is bluer at the low- and redder at the high-column-density side of the peak, respectively. These colour changes are a direct consequence of the wavelength dependence of the extinction. We have compared the colours of the LDN 1642 area with other relevant observational studies: high-latitude diffuse/translucent clouds, wide-field cirrus dust; and externally illuminated AGB-star envelopes. For extragalactic low-surface-brightness sources cirrus is an unwanted foreground contaminant. Our results for cirrus colours can help to distinguish cases where a diffuse plume or stream, apparently associated with a galaxy or a group or cluster, is more likely a local cirrus structure. Keywords: ISM: dust, extinction – ISM: clouds, individual LDN 1642 – Galaxy: solar neighbourhood – Astronomical instruments, methods and techniques: methods – Physical data and processes: scattering

35. Tidal truncation of circumplanetary disks fails above a critical disk aspect ratio

Rebecca G. Martin, Philip J. Armitage, Stephen H. Lubow, Daniel J. Price ★ We use numerical simulations of circumplanetary disks to determine the boundary between disks that are radially truncated by the tidal potential, and those where gas escapes the Hill sphere. We consider a model problem, in which a coplanar circumplanetary disk is resupplied with gas at an injection radius smaller than the Hill radius. We evolve the disk using the PHANTOM Smoothed Particle Hydrodynamics code until a steady-state is reached. We find that the most significant dependence of the truncation boundary is on the disk aspect ratio H/R. Circumplanetary disks are efficiently truncated for $H/R \lesssim 0.2$. For $H/R \simeq 0.3$, up to about half of the injected mass, depending on the injection radius, flows outwards through the decretion disk and escapes. As expected from analytic arguments, the conditions (H/R and Shakura-Sunyaev α) required for tidal truncation are independent of planet mass. A simulation with larger $\alpha = 0.1$ shows stronger outflow than one with $\alpha = 0.01$, but the dependence on transport efficiency is less important than variations of H/R. Our results suggest two distinct classes of circumplanetary disks: tidally truncated thin disks with dust-poor outer regions, and thicker actively decreting disks with enhanced dust-to-gas ratios. Applying our results to the PDS 70c system, we predict a largely truncated circumplanetary disk, but it is possible that enough mass escapes to support an outward flow of dust that could explain the observed disk size.

36. An inflationary disk phase to explain extended protoplanetary dust disks

Raphael Marschall, Alessandro Morbidelli ★ Understanding planetesimal formation is an essential first step to understanding planet formation. The distribution of these first solid bodies will drive the locations where planetary embryos can grow. We seek to understand the parameter space of possible protoplanetary disk formation and evolution models of our Solar System. A good protoplanetary disk scenario for the Solar System must meet at least the following three criteria: 1) an extended dust disk (at least 45 au); 2) formation of planetesimals in at least two distinct locations; and 3) transport of high temperatures condensates (i.e., calcium-aluminium-rich inclusion, CAIs) to the outer disk. We explore a large parameter space to study the effect of the disk viscosity, the timescale of infall of material into the disk, the distance within which material is deposited into the disk, and the fragmentation threshold of dust particles. We find that scenarios with a large initial disk viscosity ($\alpha > 0.05$), relatively short infall timescale ($T_{infall} < 100 - 200$ kyr), and a small centrifugal radius ($R_C \sim 0.4$ au; the distance within which material falls into the disk) result in disks that satisfy the criteria for a good protoplanetary disk of the Solar System. The large initial viscosity and short infall timescale result in a rapid initial expansion of the disk, which we dub the inflationary phase of the disk. Furthermore, a temperature-dependent fragmentation threshold, which mimics that cold icy particles break more easily, results in larger and more massive disks. This results in more "icy" than "rocky" planetesimals. Such scenarios are also better in line with our Solar System, which has small terrestrial planets and massive giant planet cores. Finally, we find that scenarios with large R_C cannot transport CAIs to the outer disk and do not produce planetesimals at two locations within the disk.

37. Infrared spectra of solid indene pure and in water ice. Implications for observed IR absorptions in TMC-1

Belén Maté, Isabel Tanarro, Vicente Timón, José Cernicharo, Victor J. Herrero ★ Experimental and theoretical infrared spectra, between 4000-500 cm^{-1} (2.5-20 microns), and infrared band strengths of two solid phases of indene, amorphous and crystalline, are given for the first time. The samples were generated via vapor deposition under high vacuum conditions on a cold surface. Density functional theory was employed for the calculations of the IR spectra. Lacking of previous information, a monoclinic symmetry is suggested for the theoretical crystalline phase of indene, based on the comparison of the calculated and experimental IR spectra. Assignments, based on the calculations, are given for the main indene IR absorptions. The infrared spectra of highly diluted mixtures of indene in amorphous solid water at 10 K are also provided, evidencing that the indene spectrum is not much altered by the water ice environment. These data are expected to be useful for the search of this species in the solid phase in astrophysical environments with the JWST. With the band strengths obtained in this work, and applying a simple literature model, we find that indene could represent at most 2-5 percent of the intensity of a weak absorption feature at 3.3 microns recently reported for Elias 16. A column density of (1.5 -0.6) 10^{16} cm^{-2} is estimated for indene in the ice mantles of TMC-1. It would correspond to aprox. (2 - 0.8) 10^{-2} of cosmic carbon, which is probably too high for a single small hydrocarbon.

38. The Gaia alerted fading of the FUor-type star Gaia21elv

Zsófia Nagy, Sunkyung Park, Péter Ábrahám, Ágnes Kóspál, Fernando Cruz-Sáenz de Miera, Mária Kun, Michał Siwak, Zsófia Marianna Szabó, Máté Szilágyi, Eleonora Fiorellino, Teresa Giannini, Jae-Joon Lee, Jeong-Eun Lee, Gábor Marton, László Szabados, Fabrizio Vitali, Jan Andrzejewski, Mariusz Gromadzki, Simon Hodgkin, Maja Jabłońska, Rene A. Mendez, Jaroslav Merc, Olga Michniewicz, Przemysław J. Mikołajczyk, Uliana Pylypenko, Milena Ratajczak, Łukasz Wyrzykowski, Michal Zejmo, Paweł Zieliński ★ FU Orionis objects (FUors) are eruptive young stars, which exhibit outbursts that last from decades to a century. Due to the duration of their outbursts, and to the fact that only about two dozens of such sources are known, information on the end of their outbursts is limited. Here we analyse follow-up photometry and spectroscopy of Gaia21elv, a young stellar object, which had a several decades long outburst. It was reported as a Gaia science alert due to its recent fading by more than a magnitude. To study the fading of the source and look for signatures characteristic of FUors, we have obtained follow-up near infrared (NIR) spectra using Gemini South/IGRINS, and both optical and NIR spectra using VLT/X-SHOOTER. The spectra at both epochs show typical FUor signatures, such as a triangular shaped H-band continuum, absorption-line dominated spectrum, and P Cygni profiles. In addition to the typical FUor signatures, [OI], [FeII], and [SII] were detected, suggesting the presence of a jet or disk wind. Fitting the spectral energy distributions with an accretion disc model suggests a decrease of the accretion rate between the brightest and faintest states. The rapid fading of the source in 2021 was most likely dominated by an increase of circumstellar extinction. The spectroscopy presented here confirms that Gaia21elv is a classical FUor, the third such object discovered among the Gaia science alerts.

39. Spectroscopic study of Herbig Ae/Be stars in the Galactic Anti-center region from LAMOST DR5

S. Nidhi, Blesson Mathew, B. Shridharan, R. Arun, R. Anusha, Sreeja S. Kartha ★ We study a sample of 119 Herbig Ae/Be stars in the Galactic anti-center direction using the spectroscopic data from Large sky Area Multi-Object fiber Spectroscopic Telescope (LAMOST) survey program. Emission lines of hydrogen belonging to the Balmer and Paschen series, and metallic lines of species such as FeII, OI, CaII triplet are identified. A moderate correlation is observed between the emission strengths of Hα and FeII 5169 Å, suggesting a possible common emission region for FeII lines and one of the components of Hα. We explored a technique for the extinction correction of the HAeBe stars using diffuse interstellar bands present in the spectrum. We estimated the stellar parameters such as age and mass of these HAeBe stars, which are found to be in the range 0.1 – 10 Myr and 1.5 – 10 $M_{\odot}$, respectively. We found that the mass accretion rate of the HAeBe stars in the Galactic anti-center direction follows the relation $\dot{M}_{acc} \propto M_{*}^{3.12^{+0.21}_{-0.34}}$, which is similar to the relation derived for HAeBe stars in other regions of the Galaxy. The mass accretion rate of HAeBe stars is found to have a functional form of $\dot{M}_{acc} \propto t^{-1.1\pm0.2}$ with age, in agreement with previous studies.

40. Early Planet Formation in Embedded Disks (eDisk). I. Overview of the Program and First Results

Nagayoshi Ohashi, John J. Tobin, Jes K. Jørgensen, Shigehisa Takakuwa, Patrick Sheehan, Yuri Aikawa, Zhi-Yun Li, Leslie W. Looney, Jonathan P. Willians, Yusuke Aso, Rajeeb Sharma, Jinshi Sai, Yoshihide Yamato, Jeong-Eun Lee, Kengo Tomida, Hsi-Wei Yen, Frankie J Encalada, Christian Flores, Sacha Gavino, Miyu Kido, Ilseung Han, Zhe-Yu Daniel Lin, Suchitra Narayanan, Nguyen Thi Phuong, Alejandro Santamaría-Miranda, Travis J. Thieme, Merel L. R. van 't Hoff, Itziar de Gregorio-Monsalvo, Patrick M. Koch, Woojin Kwon,

Shih-Ping Lai, Chang Won Lee, Adele Plunkett, Kazuya Saigo, Shingo Hirano, Ka Ho Lam, Shoji Mori ★ We present an overview of the Large Program, "Early Planet Formation in Embedded Disks (eDisk)", conducted with the Atacama Large Millimeter/submillimeter Array (ALMA). The ubiquitous detections of substructures, particularly rings and gaps, in protoplanetary disks around T Tauri stars raise the possibility that at least some planet formation may have already started during the embedded stages of star formation. In order to address exactly how and when planet formation is initiated, the program focuses on searching for substructures in disks around 12 Class 0 and 7 Class I protostars in nearby (<200 pc) star-forming regions through 1.3 mm continuum observations at a resolution of ~ 7 au (0.04"). The initial results show that the continuum emission, mostly arising from dust disks around the sample protostars, has relatively few distinctive substructures, such as rings and spirals, in marked contrast to Class II disks. The dramatic difference may suggest that substructures quickly develop in disks when the systems evolve from protostars to Class II sources or alternatively that high optical depth of the continuum emission could obscure internal structures. Kinematic information obtained through CO isotopologue lines and other lines reveals the presence of Keplerian disks around protostars, providing us with crucial physical parameters, in particular, the dynamical mass of the central protostars. We describe the background of the eDisk program, the sample selection and their ALMA observations, the data reduction, and also highlight representative first-look results.

41. Looking for evidence of high-mass star formation at core scale in a massive molecular clump

M. E. Ortega, N. C. Martinez, S. Paron, A. Marinelli, N. L. Isequilla ★ We present a comprehensive physical and chemical study of the fragmentation and star formation activity towards the massive clump AGAL G338.9188+0.5494 harbouring the extended green object EGO 338.92+0.55(b). The presence of an EGO embedded in a massive clump, suggests, at clump scale, that high-mass star formation is occurring. The main goal of this work is to find evidence of such high-mass star formation, but at core scale. Using mm observations of continuum and lines obtained from the ALMA database at Bands 6 and 7, we study the substructure of the massive clump. The angular resolution of the data is about 0.5", which allow us to resolve structures of about 0.01pc ($\sim$ 2000 au) at the distance of 4.4 kpc. The continuum emission at 340 GHz reveals that the molecular clump is fragmented in five cores, labeled from C1 to C5. The ^{12}CO J=3–2 emission shows the presence of molecular outflows related to three of them. The analysis of the CH_3CN and CH_3CCH emissions suggests temperatures of about 340 and 72 K, respectively, for C1, showing that the methyl cyanide would trace a gas layer closer to the protostar than the methyl acetylene. The obtained mass of core C1 ranges from 3 to 10 $M_\odot$. We found that the discovered molecular outflow arising from core C1 should be the main responsible for the 4.5 μm extended emission. The average mass and energy of such a molecular outflow is about 0.5 $M_\odot$ and 10^{46} erg, respectively, which suggest that 10 $M_\odot$ is the most likely mass value for core C1. Additionally we found that the region is chemically very rich with several complex molecular species. Particularly, from the analysis of the CN emission we found strong evidence that such a radical is indirectly tracing the molecular outflows, more precisely the border of the cavity walls carved out by such outflows.

42. Dust enrichment and grain growth in a smooth disk around the DG Tau protostar revealed by ALMA triple bands frequency observations

Satoshi Ohashi, Munetake Momose, Akimasa Kataoka, Aya E Higuchi, Takashi Tsukagoshi, Takahiro Ueda, Claudio Codella, Linda Podio, Tomoyuki Hanawa, Nami Sakai, Hiroshi Kobayashi, Satoshi Okuzumi, Hidekazu Tanaka ★ Characterizing the physical properties of dust grains in a protoplanetary disk is critical to comprehending the planet formation process. Our study presents ALMA high-resolution observations of the young protoplanetary disk around DG Tau at a 1.3 mm dust continuum. The observations, with a spatial resolution of $\approx 0.04''$, or ≈ 5 au, revealed a geometrically thin and smooth disk without substantial substructures, suggesting that the disk retains the initial conditions of the planet formation. To further analyze the distributions of dust surface density, temperature, and grain size, we conducted a multi-band analysis with several dust models, incorporating ALMA archival data of the 0.87 mm and 3.1 mm dust polarization. The results showed that the Toomre Q parameter is $\lesssim 2$ at a 20 au radius, assuming a dust-to-gas mass ratio of 0.01. This implies that a higher dust-to-gas mass ratio is necessary to stabilize the disk. The grain sizes depend on the dust models, and for the DSHARP compact dust, they were found to be smaller than ~ 400 μm in the inner region ($r \lesssim 20$ au), while exceeding larger than 3 mm in the outer part. Radiative transfer calculations show that the dust scale height is lower than at least one-third of the gas scale height. These distributions of dust enrichment, grain sizes, and weak turbulence strength may have significant implications for the formation of planetesimals through mechanisms such as streaming instability. We also discuss the CO snowline effect and collisional fragmentation in dust coagulation for the origin of the dust size distribution.

43. Constraining the gas distribution in the PDS 70 disk as a method to assess the effect of planet-disk interactions

B. Portilla-Revelo, I. Kamp, S. Facchini, E. F. van Dishoeck, C. Law, Ch. Rab, J. Bae, M. Benisty, K. Öberg, R. Teague ★ Embedded planets are potentially the cause of substructures like gaps and cavities observed in several protoplanetary disks. Thus, the substructures observed in the continuum and in line emission encode information about the

presence of planets in the system and how they interact with the natal disk. The pre-transitional disk around the star PDS 70 is the first case of two young planets imaged within a dust depleted gap that was likely carved by themselves. We aim to determine the spatial distribution of the gas and dust components in the PDS 70 disk. The axisymmetric substructures observed in the resulting profiles are interpreted in the context of planet-disk interactions. We develop a thermo-chemical forward model for an axisymmetric disk to explain a subset of the Atacama Large Millimeter/Submillimeter Array (ALMA) band 6 observations of three CO isotopologues plus the continuum towards PDS 70. Combining the inferred gas and dust distributions, the model results in a variable gas-to-dust ratio profile throughout the disk that spans two orders of magnitude within the first 130 au and shows a step gradient towards the outer disk, which is consistent with the presence of a pressure maxima driven by planet-disk interactions. We find a gas density drop factor of ∼19 at the location of the planet PDS 70 c with respect to the peak gas density at 75 au. Combining this value with literature results on the hydrodynamics of planet-disk interactions, we find this gas gap depth to be consistent with independent planet mass estimates from infrared observations. Our findings point towards gas stirring processes taking place in the common gap due to the gravitational perturbation of both planets.

44. The Origin of Chondrules: Constraints from Matrix-Chondrule Complementarity

Herbert Palme, Dominik C. Hezel, Denton S. Ebel ★ One of the major unresolved problems in cosmochemistry is the origin of chondrules, once molten, spherical silicate droplets with diameters of 0.2 to 2 mm. Chondrules are an essential component of primitive meteorites and perhaps of all early solar system materials including the terrestrial planets. Numerous hypotheses have been proposed for their origin. Many carbonaceous chondrites are composed of about equal amounts of chondrules and fine-grained matrix. Recent data confirm that matrix in carbonaceous chondrites has high Si/Mg and Fe/Mg ratios when compared to bulk carbonaceous chondrites with solar abundance ratios. Chondrules have the opposite signature, low Si/Mg and Fe/Mg ratios. In some carbonaceous chondrites chondrules have low Al/Ti ratios, matrix has the opposite signature and the bulk is chondritic. It is shown in detail that these complementary relationships cannot have evolved on the parent asteroid(s) of carbonaceous chondrites. They reflect preaccretionary processes. Both chondrules and matrix must have formed from a single, solar-like reservoir. Consequences of complementarity for chondrule formation models are discussed. An independent origin and/or random mixing of chondrules and matrix can be excluded. Hence, complementarity is a strong constraint for all astrophysical-cosmochemical models of chondrule formation. Although chondrules and matrix formed from a single reservoir, the chondrule-matrix system was open to the addition of oxygen and other gaseous components.

45. Water in the terrestrial planet-forming zone of the PDS 70 disk

G. Perotti, V. Christiaens, Th. Henning, B. Tabone, L. B. F. M. Waters, I. Kamp, G. Olofsson, S. L. Grant, D. Gasman, J. Bouwman, M. Samland, R. Franceschi, E. F. van Dishoeck, K. Schwarz, M. Güdel, P. -O. Lagage, T. P. Ray, B. Vandenbussche, A. Abergel, O. Absil, A. M. Arabhavi, I. Argyriou, D. Barrado, A. Boccaletti, A. Caratti o Garatti, V. Geers, A. M. Glauser, K. Justannont, F. Lahuis, M. Mueller, C. Nehmé, E. Pantin, S. Scheithauer, C. Waelkens, R. Guadarrama, H. Jang, J. Kanwar, M. Morales-Calderón, N. Pawellek, D. Rodgers-Lee, J. Schreiber, L. Colina, T. R. Greve, G. Östlin, G. Wright ★ Terrestrial and sub-Neptune planets are expected to form in the inner (< 10 AU) regions of protoplanetary disks. Water plays a key role in their formation, although it is yet unclear whether water molecules are formed in-situ or transported from the outer disk. So far Spitzer Space Telescope observations have only provided water luminosity upper limits for dust-depleted inner disks, similar to PDS 70, the first system with direct confirmation of protoplanet presence. Here we report JWST observations of PDS 70, a benchmark target to search for water in a disk hosting a large (∼ 54 AU) planet-carved gap separating an inner and outer disk. Our findings show water in the inner disk of PDS 70. This implies that potential terrestrial planets forming therein have access to a water reservoir. The column densities of water vapour suggest in-situ formation via a reaction sequence involving O, H_2, and/or OH, and survival through water self-shielding. This is also supported by the presence of CO_2 emission, another molecule sensitive to UV photodissociation. Dust shielding, and replenishment of both gas and small dust from the outer disk, may also play a role in sustaining the water reservoir. Our observations also reveal a strong variability of the mid-infrared spectral energy distribution, pointing to a change of inner disk geometry.

46. Alignment of dense molecular core morphology and velocity gradients with ambient magnetic fields

A. Pandhi, R. K. Friesen, L. Fissel, J. E. Pineda, P. Caselli, M. C-Y. Chen, J. Di Francesco, A. Ginsburg, H. Kirk, P. C. Myers, S. S. R. Offner, A. Punanova, F. Quan, E. Redaelli, E. Rosolowsky, S. Scibelli, Y. M. Seo, Y. Shirley ★ Studies of dense core morphologies and their orientations with respect to gas flows and the local magnetic field have been limited to only a small sample of cores with spectroscopic data. Leveraging the Green Bank Ammonia Survey alongside existing sub-millimeter continuum observations and Planck dust polarization, we produce a cross-matched catalogue of 399 dense cores with estimates of core morphology, size, mass, specific angular momentum, and magnetic field orientation. Of the 399 cores, 329 exhibit 2D v_{LSR} maps that are well fit with a linear gradient, consistent with rotation projected on the sky. We find a best-fit specific angular momentum and core size relationship of $J/M \propto R^{1.82\pm0.10}$, suggesting that core velocity

gradients originate from a combination of solid body rotation and turbulent motions. Most cores have no preferred orientation between the axis of core elongation, velocity gradient direction, and the ambient magnetic field orientation, favouring a triaxial and weakly magnetized origin. We find, however, strong evidence for a preferred anti-alignment between the core elongation axis and magnetic field for protostellar cores, revealing a change in orientation from starless and prestellar populations that may result from gravitational contraction in a magnetically-regulated (but not dominant) environment. We also find marginal evidence for anti-alignment between the core velocity gradient and magnetic field orientation in the L1228 and L1251 regions of Cepheus, suggesting a preferred orientation with respect to magnetic fields may be more prevalent in regions with locally ordered fields.

47. The multiplicity of massive stars in the Scorpius OB1 association through high-contrast imaging

Tinne Pauwels, Maddalena Reggiani, Hugues Sana, Alan Rainot, Kaitlin Kratter ★ One of the most remarkable properties of massive stars is that almost all of them are found in binaries or higher-order multiple systems. Observations that cover the full companion mass ratio and separation regime are essential to constrain massive star and binary formation theories. We used VLT/SPHERE to characterise the multiplicity properties of 20 OB stars in the active star-forming region Sco OB1. We simultaneously observed with the IFS and IRDIS instruments, obtaining high-contrast imaging observations that cover a field of view of 1".73 x 1".73 in YJH bands and 11" x 12".5 in K_1 and K_2 bands, respectively, corresponding to a separation range between ∼200 and 9000 AU. The observations reach contrast magnitudes down to $\Delta K_1 \sim 13$, allowing us to detect companions at the stellar-substellar boundary. In total, we detect 789 sources, most of which are likely background or foreground objects. We obtain SPHERE companion fractions of 2.3 ± 0.4 and 4.2 ± 0.8 for O- and B-type stars, respectively. Including all previously detected companions, we find a total multiplicity fraction of 0.89 ± 0.07 for our sample in the range of ∼0-12000 AU. In conclusion, SPHERE explores an as of yet uncharted territory of companions around massive stars, which is crucial to ultimately improve our understanding of massive star and binary formation.

48. Detection of a High-velocity Jet from MWC 349A Traced by Hydrogen Recombination Line Emission

Sirina Prasad, Qizhou Zhang, James Moran, Yue Cao, Izaskun Jimenéz-Serra, Jesus Martín-Pintado, Antonio Martinez Henares, Alejandro Báez Rubio ★ MWC 349A is one of the rare stars known to have hydrogen radio recombination line (RRL) masers. The bright maser emission makes it possible to study the dynamics of the system at milli-arcsecond (mas) precision. We present Atacama Large Millimeter/submillimeter Array (ALMA) observations of the 1.4 mm and 0.8 mm continuum emission of MWC 349A, as well as the H30α and H26α RRLs. Using the most extended array configuration of C43-10 with a maximum baseline of 16.2km, we spatially resolved the H30α line and 1.4mm continuum emission for the first time. In addition to the known H30α and H26α maser emission from a Keplerian disk at LSR velocities from -12 to 28 km s^{-1} and from an ionized wind for velocities between -12 to -40 km s^{-1} and 28 to 60 km s^{-1}, we found evidence of a jet along the polar axis at $V_{\rm LSR}$ from -85 to -40 km s^{-1} and +60 to +100 km s^{-1}. These masers are found in a linear structure nearly aligned with the polar axis of the disk. If these masers lie close to the polar axis, their velocities could be as high as 575 km s^{-1}, which cannot be explained solely by a single expanding wind as proposed in Báez Rubio et al (2013). We suggest that they originate from a high-velocity jet, likely launched by a magnetohydrodynamic wind. The jet appears to rotate in the same direction as the rotation of the disk. A detailed radiative transfer modeling of these emissions will further elucidate the origin of these masers in the wind.

49. Effect of Dust Evaporation and Thermal Instability on Temperature Distribution in a Protoplanetary Disk

Ya. N. Pavlyuchenkov, V. V. Akimkin, A. P. Topchieva, E. I. Vorobyov ★ The thermal instability of accretion disks is widely used to explain the activity of cataclysmic variables, but its development in protoplanetary disks has been studied in less detail. We present a semi-analytical stationary model for calculating the midplane temperature of a gas and dust disk around a young star. The model takes into account gas and dust opacities, as well as the evaporation of dust at temperatures above 1000 K. Using this model, we calculate the midplane temperature distributions of the disk under various assumptions about the source of opacity and the presence of dust. We show that when all considered processes are taken into account, the heat balance equation in the region r<1 au has multiple temperature solutions. Thus, the conditions for thermal instability are met in this region. To illustrate the possible influence of instability on the accretion state in a protoplanetary disk, we consider a viscous disk model with alpha parameterization of turbulent viscosity. We show that in such a model the disk evolution is non-stationary, with alternating phases of accumulation of matter in the inner disk and its rapid accretion onto the star, leading to an episodic accretion pattern. These results indicate that this instability needs to be taken into account in evolutionary models of protoplanetary disks.

50. Chemical clocks and their time zones: understanding the [s/Mg]–age relation with birth radii

Bridget Ratcliffe, Ivan Minchev, Gabriele Cescutti, Emanuele Spitoni, Henrik Jönsson, Friedrich Anders, Anna Queiroz, Matthias Steinmetz ★ The relative enrichment of s-process to α-elements ([s/α]) has been linked with age, providing a potentially useful avenue in exploring the Milky Way's chemical evolution. However, the age–[s/α] relationship is non-universal, with dependencies on metallicity and current location in the Galaxy. In this work, we examine these chemical clock tracers across birth radii (R_{birth}), recovering the inherent trends between the variables. We derive R_{birth} and explore the [s/α]–age–R_{birth} relationship for 36,652 APOGEE DR17 red giant and 24,467 GALAH DR3 main sequence turnoff and subgiant branch disk stars using [Ce/Mg], [Ba/Mg], and [Y/Mg]. We discover that the age–[s/Mg] relation is strongly dependent on birth location in the Milky Way, with stars born in the inner disk having the weakest correlation. This is congruent with the Galaxy's initially weak, negative [s/Mg] radial gradient, which becomes positive and steep with time. We show that the non-universal relations of chemical clocks is caused by their fundamental trends with R_{birth} over time, and suggest that the tight age–[s/Mg] relation obtained with solar-like stars is due to similar R_{birth} for a given age. Our results are put into context with a Galactic chemical evolution model, where we demonstrate the need for data-driven nucleosynthetic yields.

51. Survival of fossil fields during the pre-main sequence evolution of intermediate-mass stars

Dominik R. G. Schleicher, Juan Pablo Hidalgo, Daniele Galli ★ Chemically peculiar Ap and Bp stars host strong large-scale magnetic fields in the range of 200 G up to 30 kG, which are often considered to be the origin of fossil magnetic fields. We assess the evolution of such fossil fields during the star formation process and the pre-main sequence evolution of intermediate stars, considering fully convective models, models including a transition to a radiative protostar and models with a radiative core. We also examine the implications of the interaction between the fossil field and the core dynamo. We employ analytic and semi-analytic calculations combined with current observational constraints. For fully convective models, we show that magnetic field decay via convection can be expected to be very efficient for realistic parameters of turbulent resistivities. Based on the observed magnetic field strength - density relation, as well as the expected amount of flux loss due to ambipolar diffusion, it appears unlikely that convection could be suppressed via strong enough magnetic fields. On the other hand, a transition from a convective to a radiative core could very naturally explain the survival of a significant amount of flux, along with the presence of a critical mass. We show that in some cases, the interaction of a fossil field with a core dynamo may further lead to changes in the surface magnetic field structure. In the future, it will be important to understand in more detail how the accretion rate evolves as a function of time during the formation of intermediate-mass protostars, including its impact on the protostellar structure. The latter may even allow to derive quantitative predictions concerning the expected population of large scale magnetic fields in radiative stars.

52. Dark Dust III: The high-quality single-cloud reddening curve sample. Scrutinizing extinction curves in the Milky Way

R. Siebenmorgen, J. Smoker, J. Krełowski, Karl Gordon, Rolf Chini ★ The nature of dust in the diffuse interstellar medium can be best investigated by means of reddening curves where only a single interstellar cloud lies between the observer and the background source. Published reddening curves often suffer from various systematic uncertainties. We merge a sample of 895 reddening curves of stars for which both FORS2 polarisation spectra and UVES high-resolution spectra are available. The resulting 111 sightlines toward OB-type stars have 175 reddening curves. For these stars, we derive their spectral type from the UVES high-resolution spectroscopy. To obtain high-quality reddening curves we exclude stars with composite spectra in the IUE/FUSE data due to multiple stellar systems. Likewise, we omit stars that have uncertain spectral type designations or stars with photometric variability. We neglect stars that show inconsistent parallaxes when comparing DR2 and DR3 from GAIA. Finally, we identify stars that show differences in the space and ground-based derived reddening curves between 0.28 μm and the U-band or in R_V. In total, we find 53 stars with one or more reddening curves passing the rejection criteria. This provides the highest quality Milky Way reddening curve sample available today. Averaging the curves from our high-quality sample, we find $R_V = 3.1 \pm 0.4$, confirming previous estimates. A future paper in this series will use the current sample of precise reddening curves and combine them with polarisation data to study the properties of Dark Dust.

53. Gaia21bty: An EXor lightcurve exhibiting an FUor spectrum

Michał Siwak, Lynne A. Hillenbrand, Ágnes Kóspál, Péter Ábrahám, Teresa Giannini, Kishalay De, Attila Moór, Máté Szilágyi, Jan Janík, Chris Koen, Sunkyung Park, Zsófia Nagy, Fernando Cruz-Sáenz de Miera, Eleonora Fiorellino, Gábor Marton, Mária Kun, Philip W. Lucas, Andrzej Udalski, Zsófia Marianna Szabó ★ Gaia21bty, a pre-main sequence star that previously had shown aperiodic dips in its light curve, underwent a considerable $\Delta G \approx 2.9$ mag brightening that occurred over a few months between 2020 October - 2021 February. The Gaia lightcurve shows that the star remained near maximum brightness for about $4-6$ months, and then started slowly fading over the next 2 years, with at least three superimposed $\sim$1 mag sudden rebrightening events. Whereas the amplitude and duration of the maximum

is typical for EXors, optical and near-infrared spectra obtained at the maximum are dominated by features which are typical for FUors. Modelling of the accretion disc at the maximum indicates that the disc bolometric luminosity is 43 $L_\odot$ and the mass accretion rate is 2.5×10^{-5} $M_\odot$ yr^{-1}, which are typical values for FUors even considering the large uncertainty in the distance ($1.7^{+0.8}_{-0.4}$ kpc). Further monitoring is necessary to understand the cause of the quick brightness decline, the rebrightening, and the other post-outburst light changes, as our multi-colour photometric data suggest that they could be caused by a long and discontinuous obscuration event. We speculate that the outburst might have induced large-scale inhomogeneous dust condensations in the line of sight leading to such phenomena, whilst the FUor outburst continues behind the opaque screen.

54. Early Planet Formation in Embedded Disks (eDisk) V: Possible Annular Substructure in a Circumstellar Disk in the Ced110 IRS4 System

Jinshi Sai, Hsi-Wei Yen, Nagayoshi Ohashi, John J. Tobin, Jes K. Jørgensen, Shigehisa Takakuwa, Kazuya Saigo, Yusuke Aso, Zhe-Yu Daniel Lin, Patrick M. Koch, Yuri Aikawa, Christian Flores, Itziar de Gregorio-Monsalvo, Ilseung Han, Miyu Kido, Woojin Kwon, Shih-Ping Lai, Chang Won Lee, Jeong-Eun Lee, Zhi-Yun Li, Leslie W. Looney, Shoji Mori, Nguyen Thi Phuong, Alejandro Santamaría-Miranda, Rajeeb Sharma, Travis J. Thieme, Kengo Tomida, Jonathan P. Williams ★ We have observed the Class 0/I protostellar system Ced110 IRS4 at an angular resolution of 0.05″ (∼10 au) as a part of the ALMA large program; Early Planet Formation in the Embedded Disks (eDisk). The 1.3 mm dust continuum emission reveals that Ced110 IRS4 is a binary system with a projected separation of ∼250 au. The continuum emissions associated with the main source and its companion, named Ced110 IRS4A and IRS4B respectively, exhibit disk-like shapes and likely arise from dust disks around the protostars. The continuum emission of Ced110 IRS4A has a radius of ∼110 au (∼ 0.6″), and shows bumps along its major axis with an asymmetry. The bumps can be interpreted as an shallow, ring-like structure at a radius of ∼40 au (∼ 0.2″) in the continuum emission, as demonstrated from two-dimensional intensity distribution models. A rotation curve analysis on the $C^{18}O$ and ^{13}CO J = 2-1 lines reveals the presence of a Keplerian disk within a radius of 120 au around Ced110 IRS4A, which supports the interpretation that the dust continuum emission arises from a disk. The ring-like structure in the dust continuum emission might indicate a possible, annular substructure in the surface density of the embedded disk, although the possibility that it is an apparent structure due to the optically thick continuum emission cannot be ruled out.

55. How large is a disk – what do protoplanetary disk gas sizes really mean?

Leon Trapman, Giovanni Rosotti, Ke Zhang, Benoit Tabone ★ It remains unclear what mechanism is driving the evolution of protoplanetary disks. Direct detection of the main candidates, either turbulence driven by magnetorotational instability or magnetohydrodynamical disk winds, has proven difficult, leaving the time evolution of the disk size as one of the most promising observables able to differentiate between these two mechanisms. But to do so successfully, we need to understand what the observed gas disk size actually traces. We studied the relation between $R_{\mathrm{CO,\ 90\%}}$, the radius that encloses 90% of the ^{12}CO flux, and R_c, the radius that encodes the physical disk size, in order to provide simple prescriptions for conversions between these two sizes. For an extensive grid of thermochemical models we calculate $R_{\mathrm{CO,\ 90\%}}$ from synthetic observations and relate properties measured at this radius, such as the gas column density, to bulk disk properties, such as R_c and the disk mass M_{disk}. We found an empirical correlation between the gas column density at $R_{\mathrm{CO,\ 90\%}}$ and disk mass: $N_{\mathrm{gas}}(R_{\mathrm{CO,\ 90\%}}) \approx 3.73 \times 10^{21} (M_{\mathrm{disk}}/M_\odot)^{0.34}$ cm^{-2}. Using this correlation we derive an analytical prescription of $R_{\mathrm{CO,\ 90\%}}$ that only depends on R_c and M_{disk}. We derive R_c for disks in Lupus, Upper Sco, Taurus and DSHARP, finding that disks in the older Upper Sco region are significantly smaller ($\langle R_c \rangle$ = 4.8 au) than disks in the younger Lupus and Taurus regions ($\langle R_c \rangle$ = 19.8 and 20.9 au, respectively). This temporal decrease in R_c goes against predictions of both viscous and wind-driven evolution, but could be a sign of significant external photoevaporation having truncated disks in Upper Sco.

56. The GAPS program at TNG XLVII: The unusual formation history of V1298 Tau

D. Turrini, F. Marzari, D. Polychroni, R. Claudi, S. Desidera, D. Mesa, M. Pinamonti, A. Sozzetti, A. Suárez Mascareño, M. Damasso, S. Benatti, L. Malavolta, G. Micela, A. Zinzi, V. J. S. Béjar, K. Biazzo, A. Bignamini, M. Bonavita, F. Borsa, C. del Burgo, G. Chauvin, P. Delorme, J. I. González Hernández, R. Gratton, J. Hagelberg, M. Janson, M. Langlois, A. F. Lanza, C. Lazzoni, N. Lodieu, A. Maggio, L. Mancini, E. Molinari, M. Molinaro, F. Murgas, D. Nardiello ★ Observational data from space and ground-based campaigns reveal that the 10-30 Ma old V1298 Tau star hosts a compact and massive system of four planets. Mass estimates for the two outer giant planets point to unexpectedly high densities for their young ages. We investigate the formation of these two outermost giant planets, V1298 Tau b and e, and the present dynamical state of V1298 Tau's global architecture to shed light on the history of this young and peculiar extrasolar system. We perform detailed N-body simulations to explore the link between the densities of V1298 Tau b and e and their migration and accretion of planetesimals within the native circumstellar disk. We combine N-body simulations and the normalized angular momentum deficit (NAMD) analysis to characterize V1298 Tau's dynamical state and connect it to the formation history of the system. We search for outer planetary companions to constrain V1298 Tau's architecture and the extension of its primordial circumstellar disk. The high densities of V1298 Tau b and e suggest

they formed quite distant from their host star, likely beyond the CO_2 snowline. The higher nominal density of V1298 Tau e suggests it formed farther out than V1298 Tau b. The current architecture of V1298 Tau is not characterized by resonant chains. Planet-planet scattering with an outer giant planet is the most likely cause for the instability, but our search for outer companions using SPHERE and GAIA observations excludes only the presence of planets more massive than 2 M_J. The most plausible scenario for V1298 Tau's formation is that the system is formed by convergent migration and resonant trapping of planets born in a compact and plausibly massive disk. The migration of V1298 Tau b and e leaves in its wake a dynamically excited protoplanetary disk and creates the conditions for the resonant chain breaking by planet-planet scattering.

57. Do all gaps in protoplanetary discs host planets?

Anastasia Tzouvanou, Bertram Bitsch, Gabriele Pichierri ★ Following the assumption that the disc substructures observed in protoplanetary discs originate from the interaction between the disc and the forming planets embedded therein, we aim to test if these putative planets could represent the progenitors of the currently observed giant exoplanets. We performed N-body simulations assuming initially three, four, five or seven planets. Our model includes pebble and gas accretion, migration, damping of eccentricities and inclinations, disc-planet interaction and disc evolution. We locate the planets in the positions where the gaps in protoplanetary discs have been observed and we evolve the systems for 100Myr including a few Myr of gas disc evolution, while also testing three values of α viscosity. For planetary systems with initially three and four planets we find that most of the growing planets lie beyond the RV detection limit of 5AU and only a small fraction of them migrate into the inner region. We also find that these systems have too low final eccentricities to be in agreement with the observed giant planet population. Systems initially consisting of five or seven planets become unstable after ≈40Kyr of integration time. This clearly shows that not every gap can host a planet. The general outcome of our simulations - too low eccentricities - is independent of the disc's viscosity and surface density. Further observations could either confirm the existence of an undetected population of wide-orbit giants or exclude the presence of such undetected population to constrain how many planets hide in gaps even further.

58. Flow of gas detected from beyond the filaments to protostellar scales in Barnard 5

M. T. Valdivia-Mena, J. E. Pineda, D. M. Segura-Cox, P. Caselli, A. Schmiedeke, S. Choudhury, S. S. R. Offner, R. Neri, A. Goodman, G. A. Fuller ★ The infall of gas from outside natal cores has proven to feed protostars after the main accretion phase (Class 0). This changes our view of star formation to a picture that includes asymmetric accretion (streamers), and a larger role of the environment. However, the connection between streamers and the filaments that prevail in star-forming regions is unknown. We investigate the flow of material toward the filaments within Barnard 5 (B5) and the infall from the envelope to the protostellar disk of the embedded protostar B5-IRS1. Our goal is to follow the flow of material from the larger, dense core scale, to the protostellar disk scale. We present new HC_3N line data from the NOEMA and 30m telescopes covering the coherence zone of B5, together with ALMA H_2CO and $C^{18}O$ maps toward the protostellar envelope. We fit multiple Gaussian components to the lines so as to decompose their individual physical components. We investigate the HC_3N velocity gradients to determine the direction of chemically-fresh gas flow. At envelope scales, we use a clustering algorithm to disentangle the different kinematic components within H_2CO emission. At dense core scales, HC_3N traces the infall from the B5 region toward the filaments. HC_3N velocity gradients are consistent with accretion toward the filament spines plus flow along them. We found a $\sim$ 2800 au streamer in H_2CO emission which is blueshifted with respect to the protostar and deposits gas at outer disk scales. The strongest velocity gradients at large scales curve toward the position of the streamer at small scales, suggesting a connection between both flows. Our analysis suggests that the gas can flow from the dense core to the protostar. This implies that the mass available for a protostar is not limited to its envelope, and can receiving chemically-unprocessed gas after the main accretion phase.

59. Rocky sub-Neptunes formed by pebble accretion: Rain of rocks from polluted envelopes

Allona Vazan, Chris W. Ormel ★ Sub-Neptune planets formed in the protoplanetary disk accreted hydrogen-helium (H,He) envelopes. Planet formation models of sub-Neptunes formed by pebble accretion result in small rocky cores surrounded by polluted H,He envelopes where most of the rock (silicate) is in vapor form at the end of the formation phase. This vapor is expected to condense and rain-out as the planet cools. In this Letter we examine the timescale for the rainout and its effect on the thermal evolution. We calculate the thermal and structural evolution of a 10 Earth masses planet formed by pebble accretion, taking into account material redistribution from silicate rainout (condensation and settling) and from convective mixing. We find that the duration of the rainout in sub-Neptunes is on Gyr timescale and varies with envelope mass: planets with envelopes below 0.75 Earth mass rainout into a core-envelope structure in less than 1 Gyr, while planets in excess of 0.75 Earth mass of H,He preserve some of their envelope pollution for billions of years. The energy released by the rainout inflates the radius with respect to planets that start out from a plain core-envelope structure. This inflation would result in estimates of the H,He contents of observed exoplanets based on the standard core-envelope structure to be too high.We identify a number of planets in the exoplanet census where rainout may operate, which would result in their H,He contents to be overestimated by up to a factor two. Future accurate age measurements by the PLATO mission may allow the identification of planets formed

with polluted envelopes.

60. Direct images and spectroscopy of a giant protoplanet driving spiral arms in MWC 758

Kevin Wagner, Jordan Stone, Andrew Skemer, Steve Ertel, Ruobing Dong, Dániel Apai, Eckhart Spalding, Jarron Leisenring, Michael Sitko, Kaitlin Kratter, Travis Barman, Mark Marley, Brittany Miles, Anthony Boccaletti, Korash Assani, Ammar Bayyari, Taichi Uyama, Charles E. Woodward, Phil Hinz, Zackery Briesemeister, Kellen Lawson, François Ménard, Eric Pantin, Ray W. Russell, Michael Skrutskie, John Wisniewski ★
Understanding the driving forces behind spiral arms in protoplanetary disks remains a challenge due to the faintness of young giant planets. MWC 758 hosts such a protoplanetary disk with a two-armed spiral pattern that is suggested to be driven by an external giant planet. We present new thermal infrared observations that are uniquely sensitive to redder (i.e., colder or more attenuated) planets than past observations at shorter wavelengths. We detect a giant protoplanet, MWC 758c, at a projected separation of 100 au from the star. The spectrum of MWC 758c is distinct from the rest of the disk and consistent with emission from a planetary atmosphere with Teff = 500 +/- 100 K for a low level of extinction (AV<30), or a hotter object with a higher level of extinction. Both scenarios are commensurate with the predicted properties of the companion responsible for driving the spiral arms. MWC 758c provides evidence that spiral arms in protoplanetary disks can be caused by cold giant planets or by those whose optical emission is highly attenuated. MWC 758c stands out both as one of the youngest giant planets known, and also as one of the coldest and/or most attenuated. Furthermore, MWC 758c is among the first planets to be observed within a system hosting a protoplanetary disk.

61. ALMA and VLBA views on the outflow associated with an O-type protostar in G26.50+0.28

Gang Wu, Christian Henkel, Ye Xu, Andreas Brunthaler, Karl M. Menten, Keping Qiu, Jingjing Li, Bo Zhang, Jarken Esimbek ★ Protostellar jets and outflows are essential ingredients of the star formation process. A better understanding of this phenomenon is important in its own right as well as for many fundamental aspects of star formation. Jets and outflows associated with O-type protostars are rarely studied with observations reaching the close vicinity of the protostars. In this work, we report high-resolution ALMA and VLBA observations to reveal a clear and consistent picture of an outflow associated with an O-type protostar candidate in the G26.50+0.28 region. These observations reveal, for the first time, a collimated jet located in the middle of the outflow cavity. The jet is found to be perpendicular to an elongated disk/toroid and its velocity gradient. The collimated jet appears to show a small amplitude ($\alpha \approx 0\overset{\circ}{.}06$) counterclockwise precession, when looking along the blueshifted jet axis from the strongest continuum source MM1, with a precession length of 0.22 pc. The inclination of the jet is likely to be very low ($\approx 8^{\circ}$), which makes it a promising target to study its transverse morphologies and kinematics. However, no clear evidence of jet rotation is found in the ALMA and VLBA observations. The three-dimensional velocities of the water maser spots appear to show the same absolute speed with respect to different opening angles, suggesting the jet winds may be launched in a relatively small region. This favors the X-wind model, that is, jets are launched in a small area near the inner disk edge.

62. Planetesimal Accretion at Short Orbital Periods

Spencer C. Wallace, Thomas R. Quinn ★ Formation models in which terrestrial bodies grow via the pairwise accretion of planetesimals have been reasonably successful at reproducing the general properties of the solar system, including small body populations. However, planetesimal accretion has not yet been fully explored in the context of the wide variety of recently discovered extrasolar planetary systems, particularly those that host short-period terrestrial planets. In this work, we use direct N-body simulations to explore and understand the growth of planetary embryos from planetesimals in disks extending down to 1 day orbital periods. We show that planetesimal accretion becomes nearly 100 percent efficient at short orbital periods, leading to embryo masses that are much larger than the classical isolation mass. For rocky bodies, the physical size of the object begins to occupy a significant fraction of its Hill sphere towards the inner edge of the disk. In this regime, most close encounters result in collisions, rather than scattering, and the system does not develop a bimodal population of dynamically hot planetesimals and dynamically cold oligarchs, like is seen in previous studies. The highly efficient accretion seen at short orbital periods implies that systems of tightly-packed inner planets should be almost completely devoid of any residual small bodies. We demonstrate the robustness of our results to assumptions about the initial disk model, and also investigate the effects that our simplified collision model has on the emergence of this non-oligarchic growth mode in a planet forming disk.

63. Spirals and clumps in V960 Mon: signs of planet formation via gravitational instability around an FU Ori star?

P. Weber, S. Pérez, A. Zurlo, J. Miley, A. Hales, L. Cieza, D. Principe, M. Cárcamo, A. Garufi, Á. Kóspál, M. Takami, J. Kastner, Z. Zhu, J. Williams ★ The formation of giant planets has traditionally been divided into two pathways: core accretion and gravitational instability. However, in recent years, gravitational instability has become less favored, primarily due to the scarcity of observations of fragmented protoplanetary disks around young stars and low occurrence rate

of massive planets on very wide orbits. In this study, we present a SPHERE/IRDIS polarized light observation of the young outbursting object V960 Mon. The image reveals a vast structure of intricately shaped scattered light with several spiral arms. This finding motivated a re-analysis of archival ALMA 1.3 mm data acquired just two years after the onset of the outburst of V960 Mon. In these data, we discover several clumps of continuum emission aligned along a spiral arm that coincides with the scattered light structure. We interpret the localized emission as fragments formed from a spiral arm under gravitational collapse. Estimating the mass of solids within these clumps to be of several Earth masses, we suggest this observation to be the first evidence of gravitational instability occurring on planetary scales. This study discusses the significance of this finding for planet formation and its potential connection with the outbursting state of V960 Mon.

64. **Early Planet Formation in Embedded Disks (eDisk). IV. The Ringed and Warped Structure of the Disk around the Class I Protostar L1489 IRS**

Yoshihide Yamato, Yuri Aikawa, Nagayoshi Ohashi, John J. Tobin, Jes K. Jørgensen, Shigehisa Takakuwa, Yusuke Aso, Jinshi Sai, Christian Flores, Itziar de Gregorio-Monsalvo, Shingo Hirano, Ilseung Han, Miyu Kido, Patrick M. Koch, Woojin Kwon, Shih-Ping Lai, Chang Won Lee, Jeong-Eun Lee, Zhi-Yun Li, Zhe-Yu Daniel Lin, Leslie W. Looney, Shoji Mori, Suchitra Narayanan, Nguyen Thi Phuong, Kazuya Saigo, Alejandro Santamaría-Miranda, Rajeeb Sharma, Travis J. Thieme, Kengo Tomida, Merel L. R. van 't Hoff, Hsi-Wei Yen ★ Constraining the physical and chemical structure of young embedded disks is crucial to understanding the earliest stages of planet formation. As part of the Early Planet Formation in Embedded Disks Atacama Large Millimeter/submillimeter Array Large Program, we present high spatial resolution ($\sim$0.″1 or $\sim$15 au) observations of the 1.3 mm continuum and ^{13}CO J = 2-1, C^{18}O J = 2-1, and SO $J_N = 6_5$-5_4 molecular lines toward the disk around the Class I protostar L1489 IRS. The continuum emission shows a ring-like structure at 56 au from the central protostar and a tenuous, optically thin emission extending beyond $\sim$300 au. The ^{13}CO emission traces the warm disk surface, while the C^{18}O emission originates from near the disk midplane. The coincidence of the radial emission peak of C^{18}O with the dust ring may indicate a gap-ring structure in the gaseous disk as well. The SO emission shows a highly complex distribution, including a compact, prominent component at $\lesssim$30 au, which is likely to originate from thermally sublimated SO molecules. The compact SO emission also shows a velocity gradient along a slightly ($\sim 15^\circ$) tilted direction with respect to the major axis of the dust disk, which we interpret as an inner warped disk in addition to the warp around $\sim$200 au suggested by previous work. These warped structures may be formed by a planet or companion with an inclined orbit, or by a gradual change in the angular momentum axis during gas infall.

65. **Submillimeter Observations of Magnetic Fields in Massive Star-forming Region W75N**

Lingzhen Zeng, Qizhou Zhang, Felipe O. Alves, Tao-Chung Ching, Josep M. Girart, Junhao Liu ★ This paper presents the results of full polarization observations of the massive star-forming region W75N, conducted with 3 arcsec spatial resolutions at 345 GHz using the Submillimeter Array (SMA). The magnetic field structures in the dense cores of the region are derived using the linearly polarized continuum emission. The overall magnetic field strength and orientation are found to agree with those from the previous observations. The plane-of-sky (POS) component of the magnetic field in the region was calculated to be 0.8 $\pm$ 0.1 mG using the angular dispersion function (ADF) method. Further analyses involving the polarization-intensity gradient-local gravity method and H13CO+ (4-3) line data indicated that the cloud is undergoing global gravitational collapse and the magnetic field is shaped by gravity and outflows in the dense core regions.